Università degli Studi di Ferrara

DOTTORATO DI RICERCA IN
"FARMACOLOGIA ED ONCOLOGIA MOLECOLARE"

CICLO XXI

COORDINATORE Prof. Pier Andrea Borea

NEW INSIGHTS OF MIR-145 FUNCTION AND REGULATION IN HUMAN BREAST CANCER.

Settore Scientifico Disciplinare MED/06

Dottorando
Dott. Spizzo Riccardo

_____
(firma)

Tutore
Prof. Croce Carlo Maria

_____
(firma)

Anni 2006/2008

TABLE OF CONTENTS

ABSTRACT

miR-145 is down-regulated in the majority of human cancers, including breast cancer (BC). However, its role remains largely unknown. Here, I provide evidence for *miR-145* induced anti-proliferative and pro-apoptotic effect in several BC cell lines, which was not detected in BC cells lacking a functional TP53 gene and exhibiting an estrogen receptor alfa (ESR1) negative status. I found that *miR-145* anti-proliferative effects were dependent upon TP53 activation and that activation of TP53 could in turn stimulates *miR-145* expression. I also found that *miR-145* could repress the expression of ESR1 protein by direct interaction with two sites within its gene coding sequence. My findings support the existence of a positive regulatory loop where *miR-145* directly targets ESR1 and indirectly activates TP53, which in turn sustains *miR-145* expression and reinforces *miR-145* overall effects on proliferation and apoptosis.

L'espressione del miR-145 e' ridotta nella maggior parte dei tumori umani, tra cui il tumore della mammella. Nonostante cio', la sua funzione rimane per lo piu' sconosciuta a tutt'oggi. Nel corso di questa tesi, dimostrero' un effetto anti proliferativo e pro apoptotico del miR-145 in diverse linee umane di carcinoma della mammella, inoltre tale effetto risulta essere assente in linee cellulari di carcinoma della mammella senza recettore alfa dell'estrogeno (ESR1) o in cellule mancanti di TP53 funzionante. Questa evidenze preliminari hanno poi

condotto alla scoperta che l'effetto del miR-145 dipende dall'attivazione di TP53 e come a sua volta TP53 induca la trascrizione del miR-145. D'altro canto, ho dimostrato come miR-145 bersagli l'ESR1 e ne riduca l'espressione proteica e l'effetto in una cellula estrogeno dipendente mediante il legame con due siti di interazione nella regione codificante dell'ESR1. I miei risultati indicano l'esistenza nel tessuto mammario di un sistema di regolazione che controlla l'espressione di ESR1, TP53 e dello stesso miR-145.

INTRODUCTION

MicroRNAs (MiRNAs) are short (19-24 nucleotides long) non coding RNAs (ncRNAs) that are generated from longer transcripts (pre and pri-miRNA) through sequential maturation steps (1). The main known function of miRNAs is to regulate gene expression at the post-transcriptional level either by inhibiting protein translation or enhancing mRNA degradation through the binding to imperfect sequence homology sites inside the 3' untranslated region (3'-UTR) of target messenger RNAs (mRNAs) and through the recruiting of the RNA inhibitory silencing complex (RISC) to these sites (2). Other miRNA mechanisms of action, such as promoter regulation (3) and activation instead of repression of target mRNAs (4), have also been revealed. MiRNAs are involved in fundamental processes, such as embryonic development, and cell differentiation (5), where a fine regulation in time and space for the correct execution of these programs is required. Consequently, it is not surprising that alterations of miRNA expression patterns have been found in many human diseases, including cancer (6).

Numerous evidences of miRNA regulation at the transcriptional level have been already reported. For example, mirR-17-92 family is regulated by c-Myc (7), and miR-34 family is regulated by TP53 (8). Interestingly, several regulatory loops have been discovered: miR-34a itself has been shown to regulate TP53 activity (9, 10), and miR-17 family to regulate E2F1-3 (7), proving the existence of complex regulatory loops between miRNAs and transcription factors (TFs) (11).

All human tumors so far analyzed present abnormalities in miRNA expression, and signatures of miRNAs that are de-regulated in different tumors have been identified (12, 13). Among these, *miR-145* represents one of the miRNAs most commonly down regulated in various human cancers, including breast (14), colon (15), and lung (16). In particular, *miR-145* role in breast cancer (BC) merits special attention, as several lines of evidence showed that its expression is inversely correlated with BC tumor grade (17, 18), tumor size (17), and proliferation index Ki-67 (14).

BC among women is one of the most commonly diagnosed malignancies, and is the second cause of cancer death (19). Although the mortality rate from BC is decreasing, still an effective therapy has to be found. To meet this need a better understanding of BC biology is necessary. *MiR-145* functions were previously studied in colon cancer and cervical cancer cells (20, 21); however, to our knowledge, the effects of *miR-145* re-expression were not reported for BC cells. Furthermore, except for IRS-1 in colon cancer cells (22) and HOXA9 in haematopoietic lineages (23), no other *miR-145* putative target has been reported so far. Therefore, the purpose of our study was to investigate *miR-145* functions and possible mechanisms of *miR-145* down regulation in BC. Our strategy consisted of screening *miR-145* effects in six breast cancer cell lines using proliferation and apoptosis assays; through this approach we were able to identify common characteristics (i.e. ESR1 and TP53 status) that could predict the biological effect of *miR-145* restoration, novel *miR-145* targets and a mechanism of *miR-145* regulation.

RESULTS

MiR-145 impairs cell proliferation in BC cell lines by apoptotic induction.

Previous study showed that *miR-145* expression was consistently reduced in human BC samples and BC cell lines in comparison with normal breast tissue (14). I further extended these findings by analyzing via quantitative real time (qRT) PCR *miR-145* expression levels in 10 BC cell lines and in 14 BC patients. Indeed, I found a lower expression of *miR-145* in BC samples (13 time lower) and cell lines (from 150 to 700 times lower) compared to normal breast tissue (**Fig.1a-b**).

To study the effects of *miR-145* re-expression in BC cell lines, I performed an *in vitro* proliferation assay (tetrazolium colorimetric MTT assay) after transfection of precursor *miR-145* molecule (Ambion, Austin, TX). Four (MCF7, CAMA-1, MCF10A and T47D) out of six BC cell lines showed an effect after *miR-145* transfection, while MDA-MB-231 and MDA-MB-436 did not show any effect (**Fig.2**). Homogeneous transfection efficiency of *miR-145* among all cell lines was assayed and confirmed by qRT PCR (**Fig.3)**, excluding the possibility that the absence of *miR-145* effect on MDA-MB-231 and MDA-MB-436 cells was due to inefficient *miR-145* transfection. Interestingly, the *miR-145* anti-proliferative effects were only detectable in cells expressing wild type (wt) TP53 or estrogen receptor alfa (ESR1).

To evaluate if *miR-145* effect on cell proliferation was due to induction of apoptosis, I next assayed the percentage of apoptotic cells after *miR-145* transfection by AnnexinV staining at different time points. I examined CAMA-1, MCF7 and MDA-MB-231 cells, which showed decreasing anti-proliferative responses after *miR-145* transfection (**Fig.2**), being CAMA-1 the most sensible and MDA-MB-231 the most resistant. The varying percentages of early apoptotic cells (AnnexinV positive/Propidium Iodide negative cells) observed in these three cell lines were consistent with their different proliferation responses following *miR-145* restoration: CAMA-1 showed the highest induction of apoptosis (4 and 6 times at 48 and 72 hours, respectively, $p<0.05$, in duplicate experiments, n=2), MCF7 showed an intermediate induction of apoptosis (3 and 2 times at 48 and 72 hours, respectively, $p<0.05$, n=2), while MDA-MB-231 did not show any apoptotic response at any time after *miR-145* transfection (**Fig.4a**). To further confirm *miR-145* apoptosis induction in MCF7 cells, I also tested the activation of caspase 3 / 7 by a reporter assay (Promega), which proved a 2 times increase of caspase 3 / 7 activity after *miR-145* overexpression (**Fig.4b**). Taken together, these results indicate that *miR-145* restoration inhibits BC cells proliferation by increasing their apoptotic rate and that this response is common only to cells with either TP53 wt or ESR1 positive status.

***MiR-145* enhances p53 transcriptional activity and *miR-145* function depends on TP53 pathway activation.**

Considering that *miR-145* exerted its anti-proliferative/apoptotic effect only in cells TP53 wt or ESR1 positive; first, I hypothesized that *miR-145* function was dependent, at least in part, upon TP53 activation. To verify this hypothesis, I measured the expression levels of PUMA and CDKN1A/p21, two transcriptional targets of TP53 (24), after *miR-145* transfection into MCF7 cells (TP53 wt and *miR-145* responsive cells). Three independent experiments showed a two-fold increase in both PUMA and CDKN1A/p21 mRNA levels

compared to cells transfected with scrambled miRNA ($p=0.05$, $p<0.05$ respectively, n=3) (**Fig.5a)**. *MiR-145* dependent induction of PUMA was further confirmed by Western Blot (**Fig.5b**). To directly verify the dependence of cell death upon TP53 pathway activation, I co-transfected MCF7 cells with *miR-145* and short interfering RNAs (siRNAs) targeting TP53 or PUMA, a downstream effector of TP53-dependent apoptotic program (25). Twenty-four hours after transfection, a 20% increase in viability (from 43% to 64%, $p<0.05$, n=3) was observed in MCF7 cells treated with *miR-145* in association with siRNA-PUMA or siRNA-p53, compared to cells treated with *miR-145* alone (**Fig.5c)**. Our findings support the hypothesis that *miR-145* effect on cell viability relies at least in part on TP53 and the activation of its downstream targets (PUMA and p21).

TP53 induces *miR-145* expression and binds upstream of *miR-145* locus.

While studying TP53 effects on miRNA expression, He et al also reported that *miR-145*, similarly to miR-34 family members, was increased several times in an ovarian cancer cell line after adriamycin treatment (26). With these evidences in mind, I hypothesized that while *miR-145* activity was dependent on p53 activation, on the other hand TP53 could in turn regulate *miR-145* expression, similarly to other regulatory loops already described for TP53 and miR-34 family (9) as well as other miRNA/TFs (7). To test the hypothesis that TP53 regulates *miR-145*, I treated MCF7 cells with Nutlin-3, a selective activator of TP53 (27), and then measured by qRT-PCR *miR-145* expression levels. As a result, I found that *miR-145* expression was indeed increased approximately 4 times after 24 hours of Nutlin-3 treatment ($p<0.05$, n=2) (**Fig.6a)**. To validate whether TP53 induction of *miR-145* expression was at the transcriptional level through direct promoter regulation, possible TP53 binding sites (TP53bs) upstream of *miR-145* locus were investigated. By using a published database of predicted TP53bs available at UCSC Genome Browser (28), I found one predicted TP53bs 31k bps upstream of *miR-145* genomic position. Additionally, an *in silico* prediction

of TP53bs was performed, using a position weight matrix (PWM) approach (29), and scanned about 30kb upstream of *miR-145* localization and identified 55 not canonical TP53 binding sites. I next tested, by Chromatin Immuno Precipitation assay (CHIP) the TP53bs present in UCSC genome browser and 6 out of 55 TP53bs that we predicted. Specifically, 3 out of the 6 selected TP53bs had both a high quality of prediction and high conservation between human and mouse, while the remaining 3 had medium quality but were located in proximity of the *miR-145* promoter predicted by CoVote algorithm (30) (**Table 1**). One of the selected sets of primers showed a specific band by PCR amplification after ChIP in cells treated with adriamycin, that was absent in the control IgG precipitated DNA (**Fig. 6b**). These results suggest that TP53 induces *miR-145* expression and binds to a genomic region located about 11kb upstream of *miR-145*.

***MiR-145* directly targets the coding sequence of ESR1.**

Since the response to *miR-145* restoration was also correlated to ESR1 in addition of TP53 status (**Fig.1**), I also hypothesized that *miR-145* could exert its effect via modulation of ESR1 expression levels. To test whether *miR-145* could repress ESR1, I transfected MCF7 cells (ESR1 dependent) with *miR-145*, and I measured ESR1 protein levels by Western Blotting. A consistent reduction of ESR1 protein 48 hours after *miR-145* transfection was detected in three independent experiments (**Fig.7a**). I also evaluated the expression of Cyclin D1, a downstream target of ESR-1, and a parallel reduction of protein levels was detected (**Fig.7a**). Since, ESR1 has a known role in cell cycle progression (31), I anticipated that *miR-145* over-expression could affect cell cycle progression, as well. To this end, I stimulated G1 synchronized MCF7 cells with estrogen in concomitance or not with *miR-145* overexpression. I observed that *miR-145* was able to repress MCF7 cell cycle progression after estrogen stimulation (**Fig.7b**). In fact, *miR-145* transfected cells exhibited an increase of cells in G1 phase (from 43.6% to 54.4% compared to scrambled, $p<0.05$ n=2) and a

reduction of cells in G2 phase (from 23.1% to 12.8% compared to scrambled, $p<0.05$ n=2). These results support the hypothesis that *miR-145* inhibition of cell proliferation could be partly due to repression of ESR1 and its ability to promote cell cycle.

Next, I wished to clarify how *miR-145* could lead to ESR1 down-modulation. First, I interrogated several online target prediction programs (Pictar, TargetScan, Miranda, Diana-microT), but none of these identified *miR-145* binding sites within the 3'UTR of ESR1 mRNA. Before excluding the possibility of a *miR-145* direct effect on ESR1 mRNA, I evaluated whether *miR-145* was able to bind ESR1 at sites other than at its 3'UTR. In fact, although most of the miRNA binding sites have been reported in 3'UTRs (2), some recent studies described the ability of miRNAs to target mRNAs within their coding sequence (CDS) (32, 33). Hence, I tested the full-length ESR1 mRNA sequence with the RNA22 prediction program that allows the identification of possible *miR-145* binding sites also in 5'UTR and CDS (34). Three putative *miR-145* binding sites were predicted, all inside the CDS of ESR1 (**Fig. 8a**), and I cloned each one of them into pGL3 luciferase reporter vector. Two out of three caused a significant decrease of luciferase activity after *miR-145* re-expression compared to control MCF7 cells (29% and 32% decrease compared to scrambled, respectively, $p<0.05$ n=6) (**Fig. 8b**), indicating that *miR-145* can repress ESR1 expression via binding to mRNA CDS.

Previous studies have shown that miRNAs can regulate mRNA expression through the inhibition of mRNA translation or degradation of mRNA. Therefore, to understand the mechanism of ESR1 down regulation by *miR-145*, I measured ESR1 mRNA levels after *miR-145* transfection. An increased level of ESR-1 mRNA was detected concomitantly to reduction of protein levels (**Fig.8c**). Moreover, to exclude an indirect effect of *miR-145* on ESR-1 protein stability, I assessed the ratio between phosphorylated Serine-118 ESR1 (known to increase ESR1 protein stability through inhibition of proteosomal degradation (35)) and total ESR1. The ratio ESR1-pS118/ESR1 was also increased after *miR-145* treatment in comparison with control ($p<0.05$, n=3) (**Fig. 8d**), thus excluding an indirect effect of *miR-145*

in enhancing ESR1 protein degradation. Therefore, since ESR1 mRNA and ESR1 protein stability were not decreased by *miR-145* treatment, these data indicate that *miR-145* inhibits ESR1 protein expression exclusively by repression of protein translation through the interaction with two target sites within the ESR1 mRNA CDS.

Proteomic and Gene Expression Profiling after *miR-145* transfection.

In order to have a wider picture of *miR-145* effects on protein expression, I performed a proteomic analysis by reverse phase proteomic array (RPPA) (see methods for detailed procedure) after enforced expression of *miR-145* in MCF7 (*miR-145* responsive) and in MDA-MB-231 (*miR-145* resistant) cells. 109 different antibodies were used probing proteins involved in cell cycle regulation, apoptosis or tyrosine kinase signaling, and I pinpointed differentially expressed proteins between *miR-145* and scrambled expressing cells by t-test analysis. In agreement with our previous observations, ESR1 and CyclinD1 were identified as being down regulated by *miR-145* also with this complementary approach. In addition, I detected 16 differentially expressed proteins (8 down-regulated and 8 up-regulated) in MCF7 cells; conversely, in MDA-MB-231 we observed a lower number of differentially expressed proteins (only 6, and all up-regulated) (**Table 2**). Except for MEK (MAP3K1), which was up regulated by *miR-145* in MDA-MB-231, none of the differentially expressed proteins identified in MCF7 and MDA-MB-231 were present in the list of *miR-145* predicted targets, according to the miRGen predictions (http://www.diana.pcbi.upenn.edu/cgi-bin/miRGen/v3/Targets.cgi). This observation may imply that if *miR-145* has any direct effects on the observed differentially expressed proteins, it may be once again through recognitions of sequence motifs outside of the 3'UTR or by indirect mechanisms.

As the main proteomic effects were found in the *miR-145* responsive MCF7 cells, I investigated the *miR-145* effects at the transciptome level in order to further identify targets that are affected at the level of mRNA abundance. By Affymetrix gene expression profiling,

using class prediction method (a method that best accurately differentiate the two classes of samples, for further details see Methods), I found 462 probes (335 genes) differentially expressed at least two two-fold in respect with the scrambled transfected cells. Out of these, 118 probes (84 genes) were down-regulated and 344 probes (251 genes) were upregulated after *miR-145* transfection (at a P value <0.0001) (**Table 3**). ESR1 was not among these genes, further confirming its *miR-145* regulation at the translational level. Considering the downregulated genes, only 9 were among the predicted targets by DIANA miRgen and therefore, the majority of gene expression changes are likely indirect consequences of enforced expression of *miR-145*. By analyzing the global effects of *miR-145* expression on transcriptoma I examined the Gene Ontology classification and found that among the down-regulated genes the most highly enriched GO category categories was “protein binding” (p=6.2E-5), while among the up-regulated genes was “immune system” (p=2.8E-28). Interestingly, for the latter group of genes, we also identified the “P53 signaling pathway” (p=2.7E-2), “apoptosis” (p=6.9E-6) or “regulation of apoptosis” (p=1.8E-4) By further checking the list of differentially expressed genes I found that TRIM 25 is involved in estrogen responsive control of cell cycle and breast tumors growth according to BioCarta pathways and that CAV2 is involved in response to estrogen stimulus according to GO biological processes. All these findings support a model depicting *miR-145* at the interface between TP53 pathway and estrogen pathway in breast cancer, expanding the already growing spectrum of examples of non-codingRNAs and protein coding genes interplay in fundamental cellular pathways (**Fig. 9**, see also discussion).

DISCUSSION

My findings indicate that *miR-145* inhibits proliferation and induces apoptosis of BC cells through the activation of TP53 pathway and the down regulation of ESR1. To my knowledge, these results describe for the first time a tumor suppressor function of *miR-145* in BC cells and directly link *miR-145* to ESR1 and TP53, both important players in breast tumor biology (36, 37).

Several papers already identified miRNAs regulated by TP53 (26, 38). He et al., using real time PCR, reported an increase of *miR-145* after TP53 activation by adriamycin in an ovarian cancer cell line (26). However, they did not see any difference in *miR-145* expression between TP53 wt and TP53 null primary mouse fibroblasts, suggesting that *miR-145* regulation by TP53 may be tissue or cell-type specific. Given this premise, the screening of different types of cell lines for *miR-145* effects may help to identify pathways and biological outcomes associated with *miR-145* expression.

It should be mentioned that *miR-145* is located at chromosome 5q33.1 in cluster with miR-143, suggesting that miR-143 is also likely regulated by TP53 together with *miR-145*. However, in the cell lines that I used, miR-143 exhibited an expression lower than *miR-145* (10 to 100 times) (**Fig.1a**), making difficult to obtain consistent results on mir-143 regulation by TP53 (data not shown).

Our findings indicate that ESR1 could play a pivotal role in a regulatory loop between *miR-145* and TP53. In fact, it has been demonstrated that ESR1 can directly interact with

TP53 protein and inhibit TP53 activity without affecting TP53 protein levels (39); therefore, it is plausible that *miR-145*, by downregulating ESR1, could indirectly induce TP53 activity without affecting TP53 protein levels. Consistent with this model, when I tested if TP53 activation by *miR-145* was dependent on an increase of TP53 protein levels, the results were inconsistent, and only in synchronized cells after estrogen stimulation we were able to see an induction of TP53 protein levels with consequent activation of p21 (**Fig. 10**).

Previous studies have described for *miR-145* a direct correlation with ESR1 tumor status (17, 18, 40) and an inverse correlation with the Ki-67 proliferation index (14). While the latter finding is in agreement with *miR-145* anti-proliferative effect that I described here with our BC cell line screening, unexpected and more difficult to explain is the direct correlation between *miR-145* and ESR1 expression levels. Distinct groups have identified other miRNAs that directly target ESR1 (miR-221, miR-222 and miR-206) (41, 42), and also for mir-221/222 a direct correlation with ESR1 status was found (40). These direct correlations although puzzling and contradictory seems to be true for multiple miRNAs that target ESR1 and not only for *miR-145*.

In conclusion, the effects on proliferation and apoptosis induced by *miR-145* re-expression support a tumor suppressor role of *miR-145* in BC pathogenesis (14, 15, 21). In fact, either in ER positive BC cells, or in BC cells carrying wt TP53, *miR-145* inhibited cell cycle progression and promoted apoptosis. In the present study, I could delineate a positive regulatory feedback loop, where *miR-145*, by targeting ESR1 mRNA and inducing ESR1 protein down-regulation, is at least in part responsible for the activation of TP53. In turn, TP53 activates its downstream effectors (PUMA and p21) as well as *miR-145* itself, thus reinforcing this positive loop, which is responsible for the overall effects on BC cell proliferation and apoptosis (**Fig.9)**. The finding that *miR-145* regulates both ESR1 and TP53 in BC cells provide a deeper insight into the involvement of *miR-145* in BC pathogenesis, and could open the avenue of new therapeutic options by the modulation of *miR-145* expression in BCs.

MATERIALS AND METHODS

MicroRNA precursor molecules and siRNAs. Synthetic microRNA precursor molecules and negative control #1 or #2 (scrambled) were purchased form Ambion (Austin, TX). The synthetic oligos were dissolved in nuclease free water to a stock concentration of 50μM. Small interfering RNA (siRNA) against TP53 and PUMA were purchased from Dharmacon (Thermo Scientific, MA, USA).

Hormones and Drugs. 17 β estradiol was purchased from Sigma Aldrich (St.Louis, MO, USA) and was dissolved in ethanol to a final concentration of 50mg/mL. Nutlin-3 was purchased from Cayman Chemical (Ann Arbor, MI, USA) and dissolved in DMSO to a stock solution of 2mM. Adriamycin was a kind gift from by Dr. Priebe's lab at MD Anderson Cancer center, Houston, TX and was resuspended in water to a final concentration of 0.5uM.

Cell lines and patient samples. MCF-7, CAMA-1, MDA-MB-231, MCF-10A, T47D, MDA-MB-436, HCT116 cell lines were obtained from the American Type Culture Collection (Manassas, VA) and cultured according to protocols. The normal breast tissues and breast cancer samples were collected and processed as described by Iorio et al (14).

Real Time PCR and RNA isolation. The RNA purification by Trizol was performed as described by Iorio et al. (14). For mature microRNA quantification, I used *miR-145* probe

(Applied Biosystems Foster City, CA) and RNU6B probe (Applied Biosystems). I used 500 ng of total RNA for retrotranscription, multiplexing two different primers (*miR-145* and RNU6B). The delta Ct method was used to calculate the relative abundance of microRNAs compared to RNU6B expression (43). To generate total cDNA for protein coding gene expression, 1ug of total RNA was retrotranscribed by SuperScript II (invitrogen, Carlsband, CA, USA) with random hexamers according to the manufacturer's protocol. The Real Time PCR was performed with iQ Syber green Supermix (Biorad). Primer list is shown in **Table 4**.

Protein isolation, Western Blotting and antibodies. Cells were collected by trypsin-EDTA (Mediatech) and dissolved in NP40 lysis buffer (0.5% NP40, 250mM NaCl, 50mM Hepes, 5mM EDTA and 0.5mM EGTA) freshly supplemented with Complete inhibitor (Roche) and phosphatase inhibitor cocktail 1&2 (Roche). Proteins were purified as previously described (44). The following antibodies were used for western blotting: ESR1 (Neomarker), ESR1 pS118 (Epitimics), GAPDH (Calbiochem), CYCLIND1 (Santa Cruz Biotechnologies), and PUMA antibody (Cell Signaling).

Reverse Phase Proteomics Assay. MCF7 and MDA-MB-231 cells were seeded in 6-well plates and transfected either with *miR-145* precursor (Ambion, Austin, TX) or with scrambled controls (Ambion, Austin, TX). Each experiment was performed in triplicate. Cells were lysed in 6-well plates and denatured by SDS at 36 hours after transfection as previously described (45). Cell lysates were serially diluted to define the linear range of each antigen-antibody reaction. Lysates were printed on nitrocellulose-coated slides and serially probed with antibodies**.** Signals were captured by tyramide dye deposition (CSA System, DAKO). Data were collected and analyzed using Biometric Research Branch (BRB) array tools 3.6.1 (http://linus.nci.nih.gov/BRB-ArrayTools.html). Class comparison analysis using *t* test identified probe sets that were differentially expressed between controls and treated samples ($P < .05$).

Expression profiles after *miR-145* transfection. MCF7 cells were starved and transfected either with *miR-145* precursor or with scrambled controls (Ambion, Austin, TX) as described in "ESR1 function, cell cycle" paragraph. After 24 hours, the cells were released using DMEM medium with 10% of fetal bovine serum. The total RNA was extracted by Trizol method (Invitrogen, Carlsband, CA, USA) and the hybridization was performed on Affymetrix array HG-U133 plus 2.0. GeneChips (Santa Clara, CA) in duplicate. The data were normalized by GCRMA and imported into Biometric Research Branch (BRB) array tools 3.6.1 (http://linus.nci.nih.gov/BRB-ArrayTools.html) for subsequent analyses. Class prediction algorithms in BRB array tools were used to determine whether genes expression patterns could accurately differentiate between control and treated samples.

***In vitro* proliferation assay.** Cells were plated in 96-well plates at a density of 10,000cells/well. The transfection was performed by Lipofectamine2000 protocol (Invitrogen, CA, USA) with a final concentration of 100nM for both *miR-145* precursor and negative control molecule (scrambled). We also treated cells with lipofectamine only (null cells). Both treatment and controls were performed in 4 replicate each time. After four hours from the transfection (time 0), the adsorbance of cells was estimated by colorimetric assay (MTT, CellTiter96Aqueous One solution, Promega, WI, USA) and the reading was repeated every 24 for four consecutive days.

Apoptotic assays. The number of early apoptotic cells was obtained by Annexin V staining kit (BD Pharmingen, 556547, San Jose, CA, USA). Every 24h, the cells were collected and Annexin V staining performed according to the protocol. The cells were counterstained with Propidium Iodide (PI) and immediately read with a FACSCalibur system (BD). Only cells Annexin V + and PI – were counted for each time points. For further confirmation, we performed for MCF7 cells the Caspase3/7 assay according to the manufacturer protocol (Promega, WI, USA).

***MiR-145* - TP53 loop identification**. MCF7 were seeded in 24-well plates at concentration of $75x10^3$ cells/well into antibiotic-free medium. Transfection was performed using Lipofectamine 2000 Reagent (Invitrogen). *MiR-145* precursor (Ambion), Negative Control#2 (Ambion), siRNA-PUMA (Dharmacon) and siRNA-p53 (Dharmacon) were transfected at final concentration of 100nM. After 48h I counted the number of cells using hemocytometer chamber. To test the effect of Nutlin-3 on *miR-145* expression in MCF7, I treated MCF7 for 24h at increasing concentration of the drug (2, 4 and 8 microM).

***In silico* identification of TP53 binding sites.** P53 binding sites were predicted by position weight matrix (PWM) approach (29) by scanning a 30 kb region upstream of *miR-145* genomic location.

Chromatin Immunoprecipitation (CHIP). HCT116 cells were plated in 175 cm^2 dish and were treated for 24 hours with Adriamycin to induce TP53 activation. CHIP was performed using CHIP kit (Millipore, cat number 17-295, USA), and 5 μg of antibody against TP53 (Santa Cruz Biotechnology). As negative control we immunoprecipitated one sample with 5 μg of pre-immune serum (Santa Cruz). After final elution and purification of DNA, the samples were PCR amplified using the primers listed in Supplementary Table S2. The input sample was diluted to 0.1ng/μL and used as positive control of PCR reaction. PCR was performed using AmpliTaq Gold (Applied Biosystems).

ESR1 Function, cell cycle analysis. $0.5x10^6$ MCF7 cells were plated in 6 well plates and starved for 44h in phenol red free DMEM and supplemented with charcoal treated FBS. Cells were then transfected with *miR-145* precursor or scrambled molecules as previously described; after 4 hours (time 0), the media was changed and replaced with fresh phenol red free DMEM, supplemented with charcoal treated FBS and 17 β estradiol (10^{-6} M). At time 0

hour and after 24 hours, the cells were collected, washed with PBS, fixed with ethanol, and stained with PI supplemented with RNse A. Both samples were analyzed together, and the same arbitrary gates for sub-G1, G1, S and G2 were used at both times 0 and 24 hours, respectively. Each transfection was performed in duplicates.

Luciferase assay. I designed three primer pairs (Table 4) to amplify a region of about 200-300 bps around every predicted *miR-145* target site within ESR1 coding sequence (CDS). The cloning of the three amplicons was done as previously described (44). $0.2x10^6$ MCF7 were plated on 24 well plates, and the day after, the cells were transfected with *miR-145* or scrambled (100 nM), with each single pGL3 ESR1 construct (0.4μg per well) and with pRLTK (0.05μg per well). After 24h the cells were rinsed with PBS and dissolved in Passive Lysis Buffer 1X (Promega). Subsequently, 20μL of samples were measured for luciferase activity using dual luciferase kit (Promega) and were read with Veritas luminometer (Turner Biosystems, Sunnyvale, CA, USA). Each combination was tested in four replicates in two independent experiments.

Statistical analysis. The t-test was used to compare average values between groups of samples (such as miRNA expression data, number of proliferating cells, etc). All reported P-values were calculated for groups with unequal variance using Excel software.

FIGURES AND TABLES

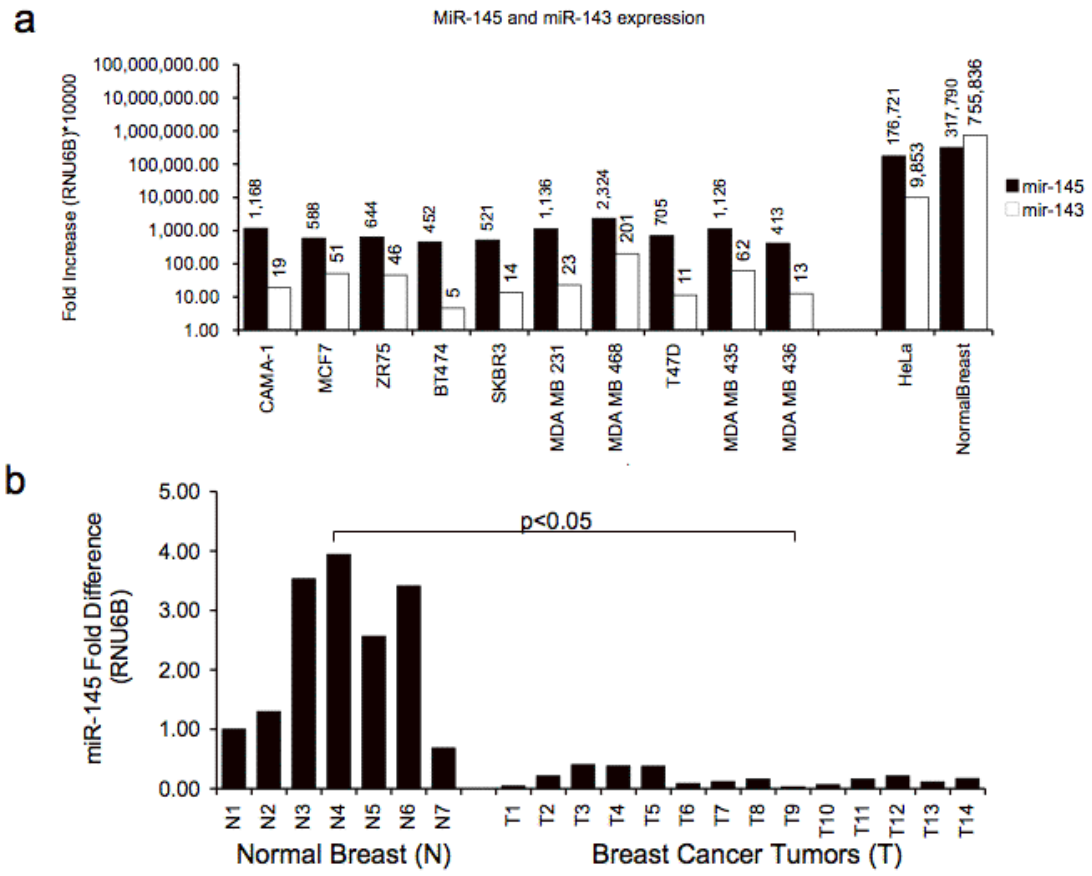

Figure 1. (a). **MiR-145 expression in breast cancer cell lines**. The expression of miR-145 was tested by real time PCR for mature miRNAs. The average expression of miR-145 in breast cancer cell lines is hundreds times less compared to Normal Breast (Ambion, Austin, TX, USA) and HeLa. Y-axis represents logarithmic fold increase compared to house keeping gene RNU6B. **(b)** miR-145 expression in BC tumors. MiR-145 was tested by real time PCR, as well. BC tumors (n=14) presented lower miR-145 expression than normals (n=7). P-value is obtained by t-test allowing unequal variance between groups.

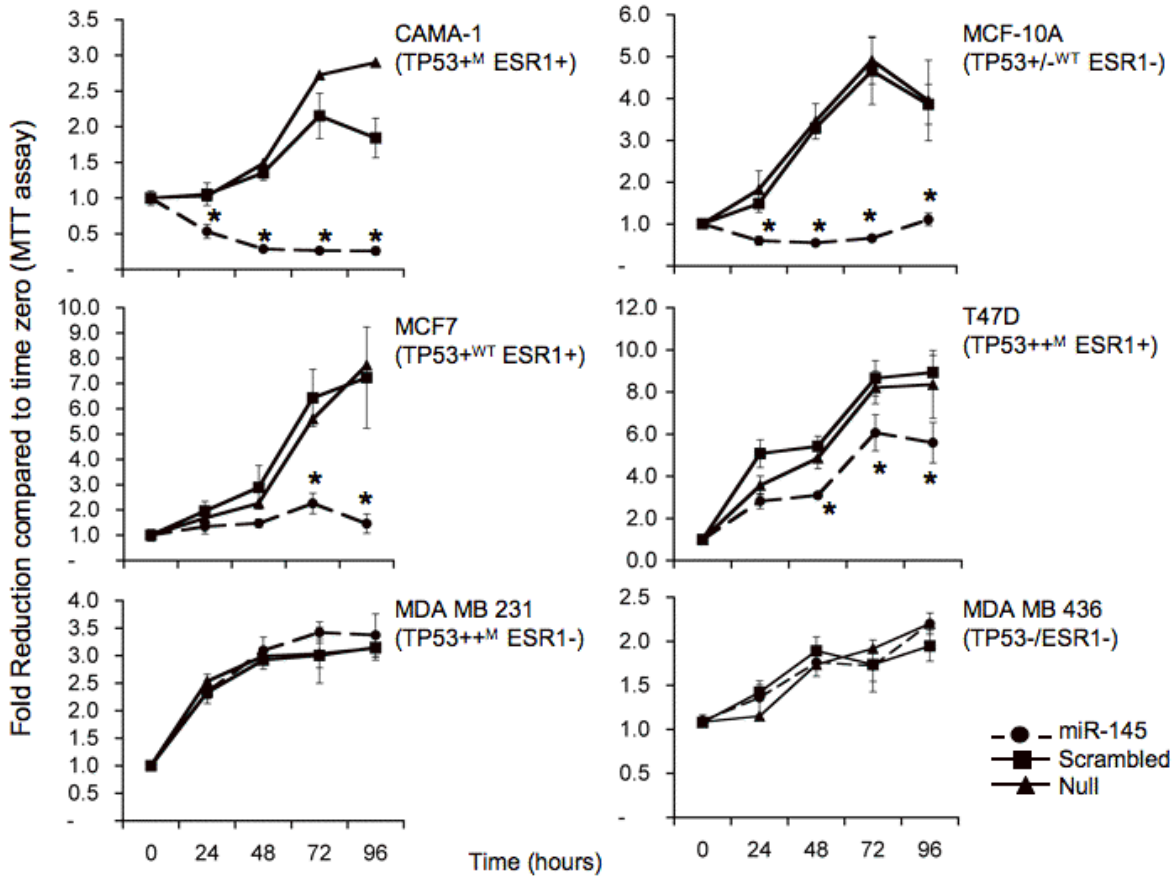

Figure 2. *MiR-145* inhibits breast cancer cell proliferation. *MiR-145* effects on proliferation and cell viability of 6 breast cancer cell lines were measured by MTT assay. Time zero corresponds to transfection day. Each time point was expressed as a relative value (Fold Increase, Y axis) to time zero. Values represent the average of 3 (MCF7 and MDA-MB-231) or 2 (all other cell lines) independent experiments, performed in quadruplicates; bars indicate standard deviations. For each cell line TP53 and ESR1 protein status are shown according to Neve et al [61]. For TP53: – indicates no expression, ++ high expression, M=mutated or WT=wild type. For ESR1, protein levels are indicated as + positive or – negative. *MiR-145* had an anti-proliferative effect only on breast cancer cell lines either expressing WT TP53 or ESR1.

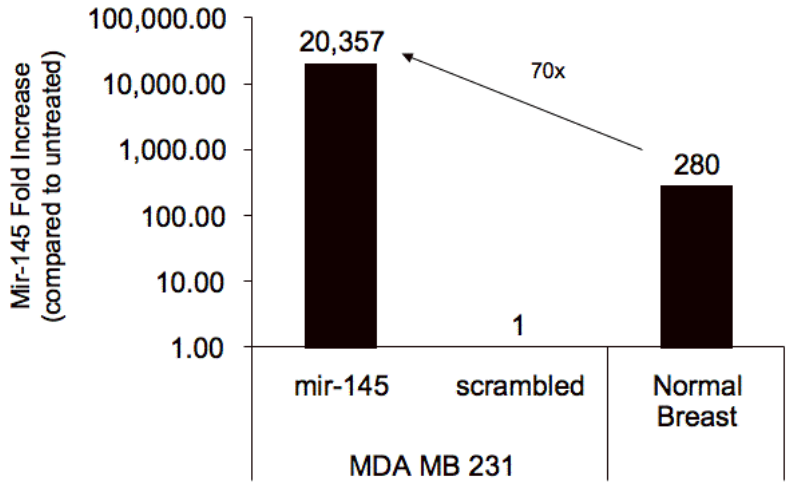

Figure 3. Testing the efficiency of miR-145 transfection. To test if miR-145 did not show any effect in MDA MB 231 because of a poor efficiency of transfection, I measured the miR-145 levels in MDA MB 231. The levels of miR-145 were consistently increased after transfection compared to scrambled transfected cells. I used the same samples as for the apoptotic assay reported in Fig. 4a.

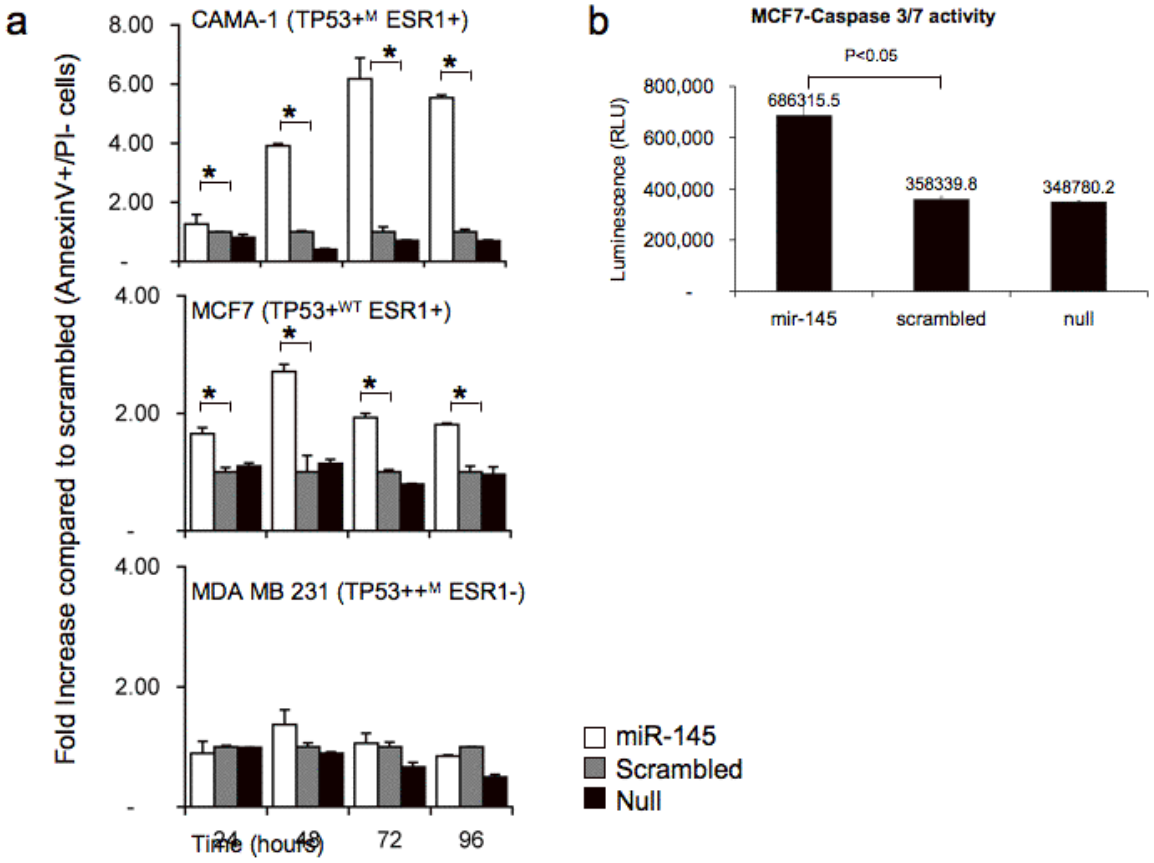

Figure 4. *MiR-145* induces breast cancer cell apoptosis. (a) AnnexinV staining of breast cancer cell lines at different time points after *miR-145* transfection. For each time point, the percentage of AnnexinV positive/Propidium Iodide (PI) negative cells after *miR-145* transfection was expressed as Fold Increase compared to scrambled transfected cells (Y axis). Values represent averages and bars standard deviation of 2 independent experiments. X-axis represents hours after transfection. *MiR-145* induced an increase of early apoptosis in CAMA-1 and MCF7 cell line, while it had no effect in MDA-MB-231. **(b)** Caspase 3/7 activity after miR-145 transfection in MCF7 cells. A two-fold increase in the activity was found in comparison with both scrambled transfected and non-transfected cells. These data further confirm the data from Fig 1B by using a different assay.

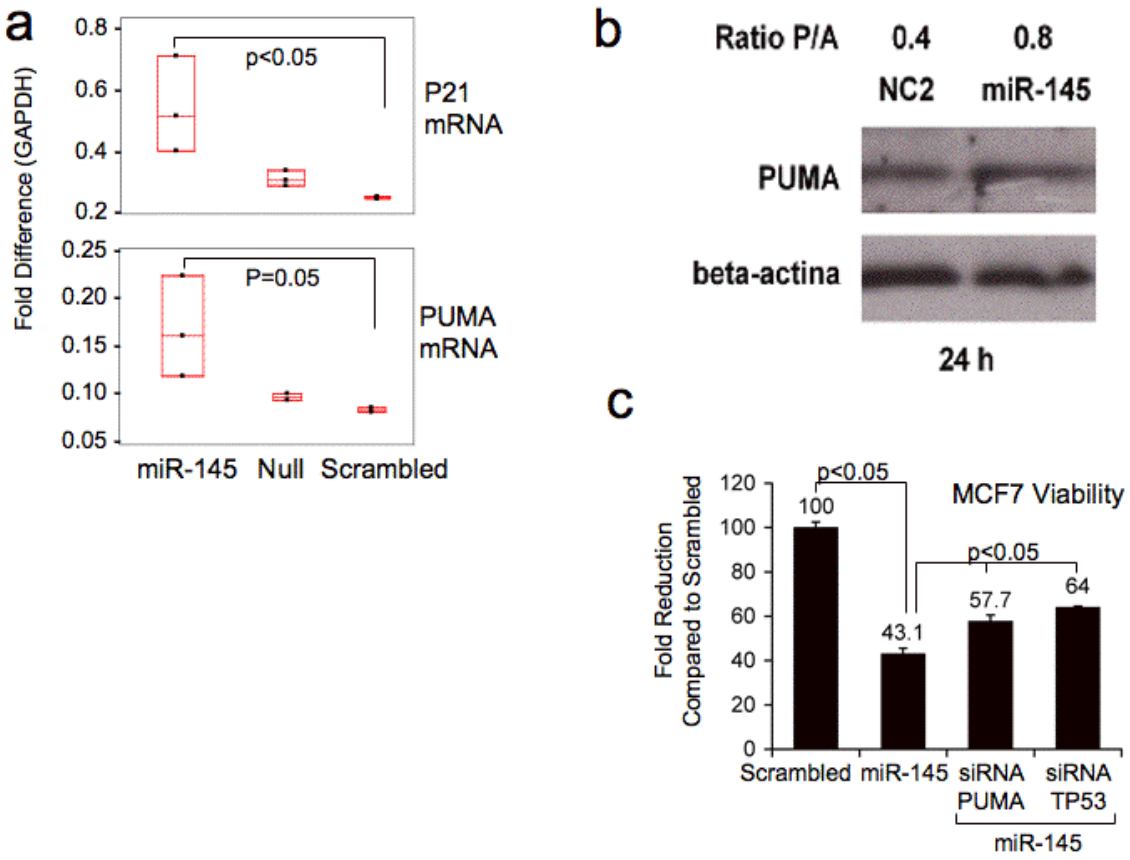

Figure 5. *MiR-145* induces TP53 activity, and *miR-145* effects depend on TP53 pathway. (a) Levels of PUMA and p21 mRNA, both downstream targets of TP53, are upregulated by *miR-145* overexpression as indicated by qRT analysis of *miR-145* transfected cells (n=3, mean ±st.dev.). **(b)** Western Blotting of PUMA in MCF7 after miR-145 transfection. MiR-145 induced an increase (0.8 versus 0.4 relative units) of PUMA protein compared to control (NC2) after 24 hours from the transfection. Top figure, PUMA antibody western blotting is shown; bottom figure, beta-actin is shown. Ratio P/A indicates PUMA values after quantification of western blotting bands and normalization with beta-actin expression. **(c)** Assessment of MCF-7 cell viability by MTT assay 48 h after *miR-145* transfection in the presence or absence (by siRNA) of TP53 or of the TP53 transcriptional target PUMA. Mean viability (n=3, ±st.dev.) of scrambled transfected cells was set to 100%. *MiR-145* induced a decrease in MCF7 cell proliferation (as shown in figure 1a, middle left panel), but this effect was reduced in the absence of PUMA or TP53.

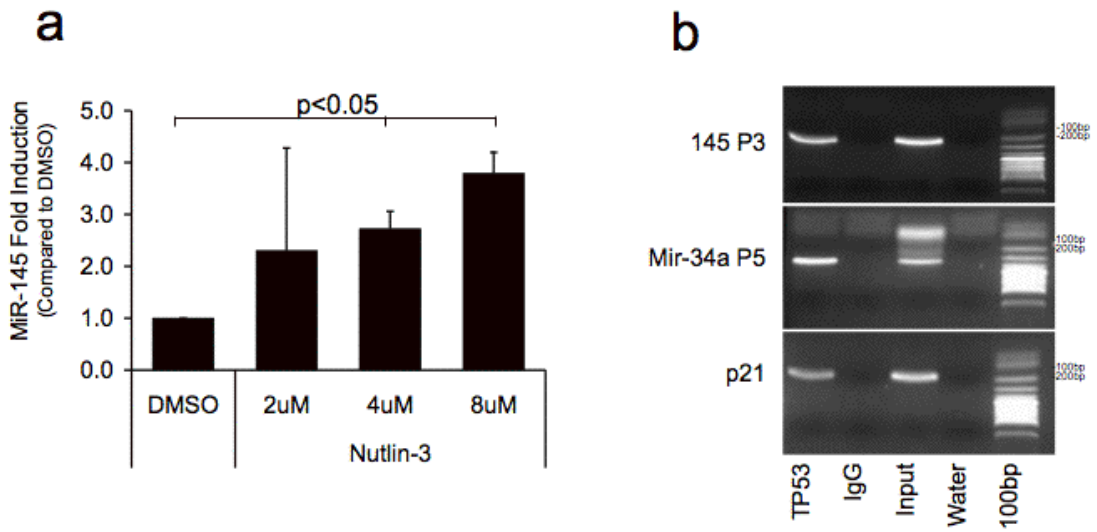

Figure 6. TP53 regulates *miR-145*. (a) *MiR-145* was induced after treatment with increasing concentration of Nutlin-3 (2, 4, 8 μM). *MiR-145* expression levels were quantified by qRT. Mean expression value (n=2, mean±st.dev.) of *miR-145* in DMSO treated cells was set to one. **(b)** The TP53 binding site (145 P3) upstream *miR-145* gene was confirmed by chromatin immuno precipitation (CHIP) analysis. A band was detected by PCR when the 145 P3 set of primers was used after IP with TP53 antibody (lane labeled as TP53), while no band was detected if pre immune serum was used for IP (lane labeled as IgG). The band was purified from the gel and the sequence was confirmed (data not shown). MiR-34a P5 [49] and p21 [50] set of primers were used as positive controls for CHIP of TP53. Rabbit pre serum IgG (IgG) was used as negative control for CHIP analysis, while genomic DNA before CHIP was used as PCR positive control (input).

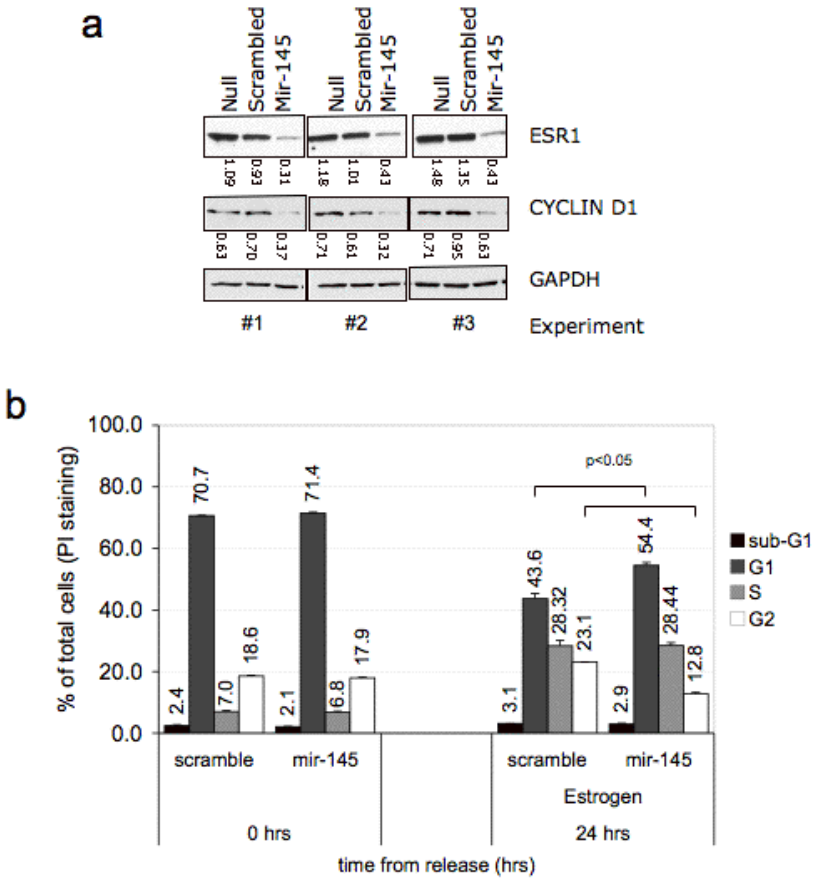

Figure 7. *MiR-145* represses ESR1 protein and inhibits estrogen function in MCF7. (a) WB analysis of ESR-1 and Cyclin D1 levels in MCF7 after *miR-145* transfection. GAPDH was used as loading control. On the top of the figure, treatments are shown (*miR-145*, scrambled and null). Under each lane, the numbers identify the band quantification after GAPDH normalization. Three independent experiments are shown. Null samples were treated only with Lipofectamine. (**b).** *MiR-145* effects on cell cycle distribution after 17-β-estradiol stimulation of synchronized MCF7 were measured by PI staining and FACS analysis of cells DNA content. 24 hours after 17-β-estradiol stimulation, *miR-145* expressing cells presented an higher percentage of cells in G1 (54.4% versus 43.6%) and lower percentage in G2 (12.8% versus 23.1%) compared to scrambled transfected cells; instead, before 17-β-estradiol stimulation (time 0 hours) no significant differences were observed. On the y-axis, the percentage of cells in each phase of the cell cycle over the total number is shown. Numbers labeling each bar identify exact percentages from 2 duplicates (mean±st.dev.). P-values were obtained by comparison of cell cycle phases between *miR-145* and scrambled transfected cells using t-test with unequal variance between groups.

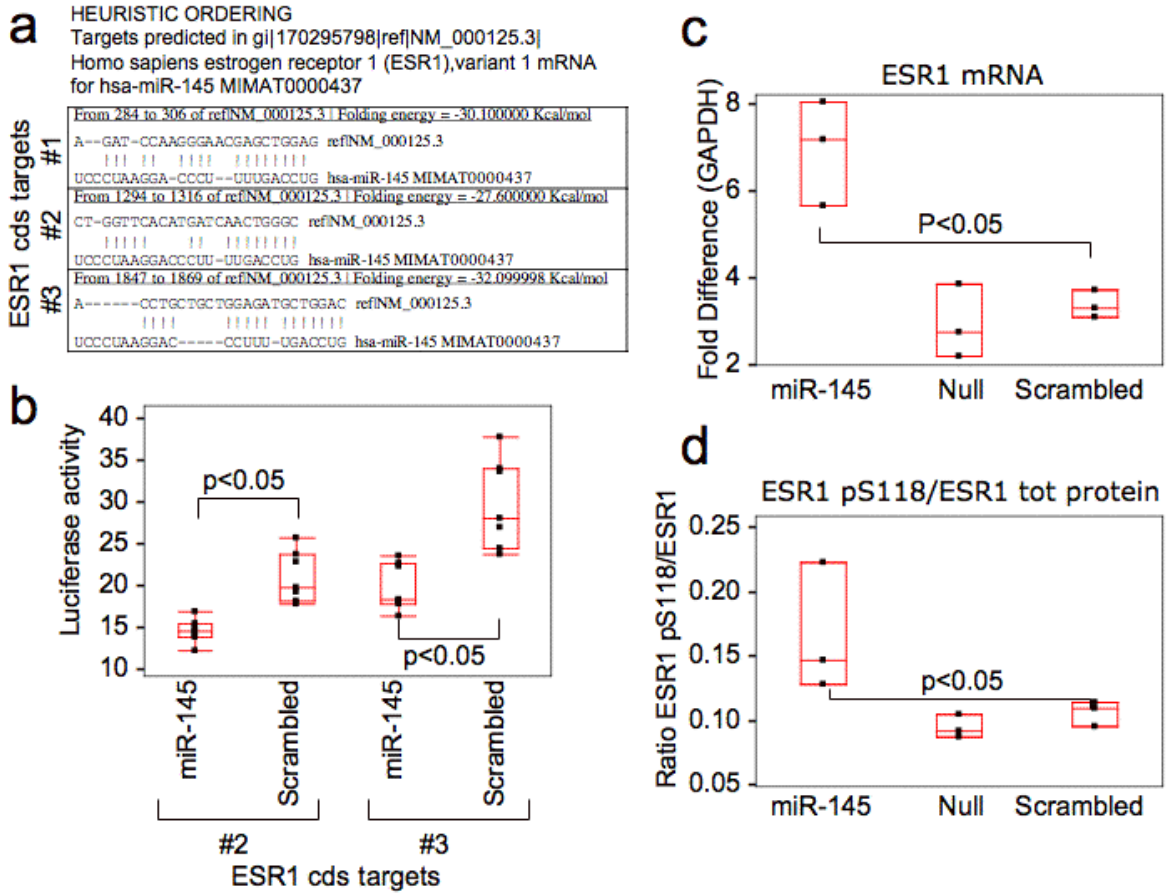

Figure 8. *MiR-145* directly targets ESR1 and regulates its expression at the translational level. **(a)** RNA22 predictions of three *miR-145* interactions sites inside ESR1 CDS (coding sequence). In each square ESR1 target site is above and *miR-145* sequence below. Vertical lines identify nucleotides of interaction. **(b)** Two of the *miR-145* binding sites inside ESR1 CDS mediate *miR-145* control of ESR1 expression. *MiR-145* inhibited luciferase activity of pGL3 constructs containing two of the three predicted *miR-145* binding sites. Luciferase activity was expressed as arbitrary units (Y axis) (ratio of Luciferase/Renilla, using pRLTK Renilla expressing vector as an internal standard). **(c)** and **(d)** ESR1 mRNA and ESR pS118/ total ESR1 were measured after *miR-145* overexpression in the same set of transfected cells used in figure 3a for ESR1 protein expression. **(c)** *MiR-145* increases significantly ESR1 mRNA levels compared to controls, as by qRT analysis. **(d)** *MiR-145* enhances ESR1 phosphorilation at Serine 118. The ESR pS118/ total ESR1 ratio was obtained from WB band quantification followed by dividing ESR1 pS118 levels by total ESR1 levels after normalization with GAPDH. P-values are obtained by t-test with unequal variance between groups.

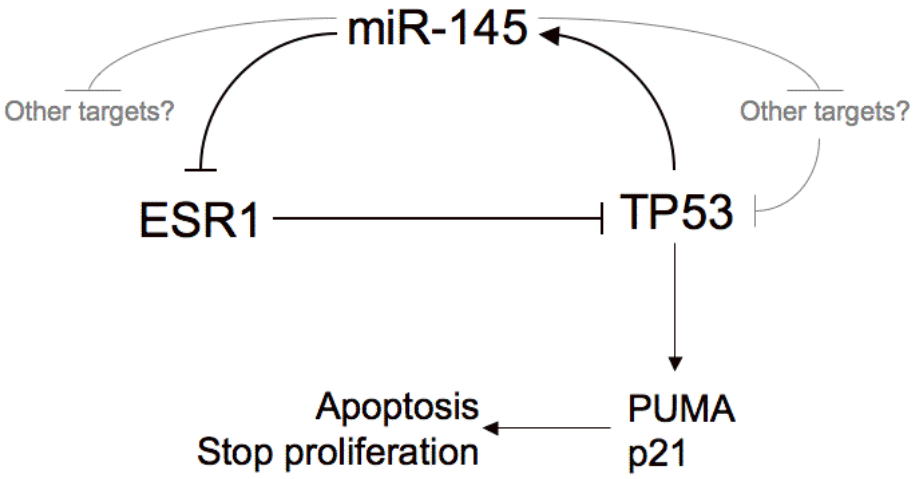

Figure 9. *MiR-145* at the center of TP53 and ESR1 effects on cell proliferation and apoptosis. A model depicting the *miR-145* regulation of TP53 pathway by inducing several members of the pathway and the estrogen pathway by targeting ESR1 and other related proteins.

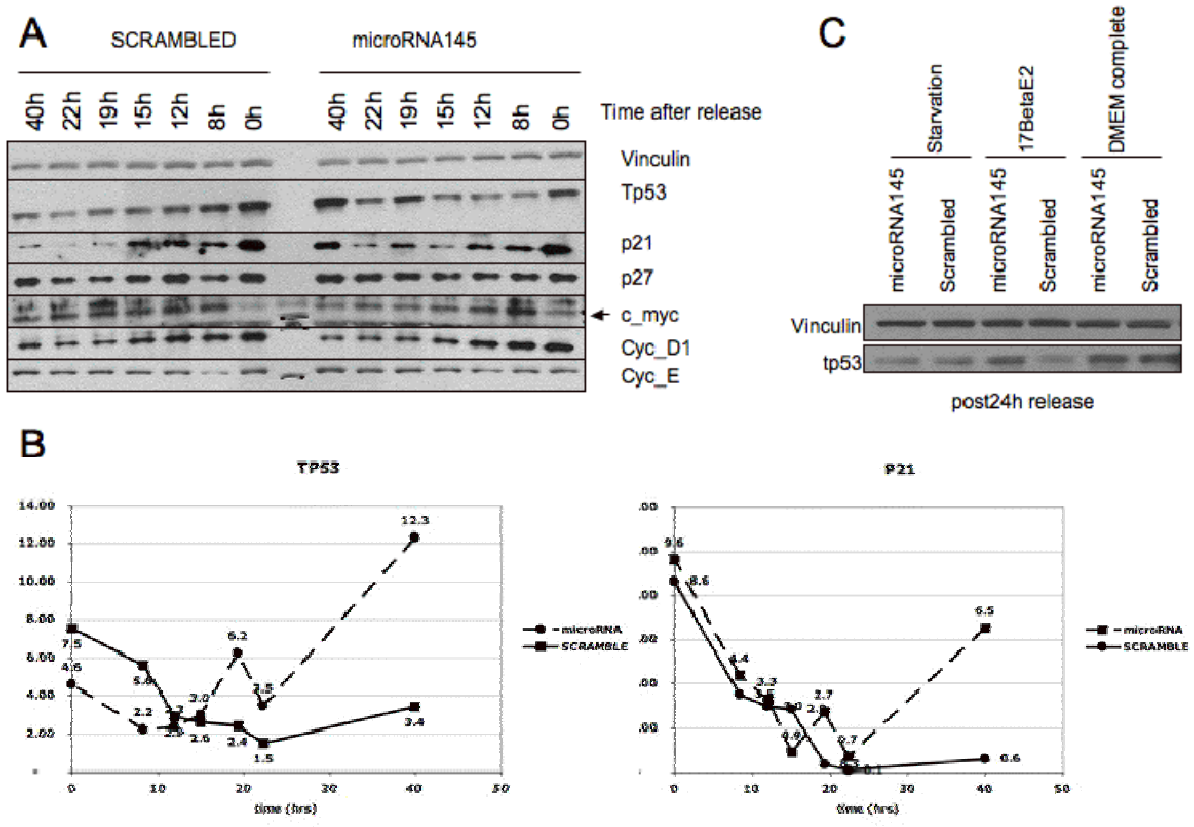

Figure 10. *MiR-145* affects TP53 protein level. (a). MCF7 cell lines were starved for 44 hours with hormone deprived bovine serum; thereafter, the cells were transfected with miR-145 or scrambled control, and after 4 more hours the cells were released with 17 beta estradiol. At different time points the cells were collected (as indicated in the top part of the figure) and protein extract was prepared. Different antibodies were tested (as listed on the right side of the picture). Vinculin was used as loading control. **(b).** After normalization, TP53 and P21 protein expression were plotted (X-axis time points, Y-axis relative values compared to vinculin). MiR-145 determined an increased of TP53 protein expression about 15 hours after release compared to scrambled control, P21 protein (a downstream target of TP53) showed a similar pattern. **(c).** In a independent experiment the same result was obtained, but only after 17 beta estradiol release, in fact neither release with complete medium (fetal bovine serum) nor starvation (charcoal treated serum) were able to induce TP53 induction after miR-145 treatment.

Table 1. TP53 binding sites used for CHIP assay.

Primer ID	Start (hg18 chr5)	End (hg18 chr5)	Distance from mir-145 (bp)	Sequence of predicted TP53 binding site	Quality
145 P1	148764176	148764197	26226	GGGCTTtCTg(0.48) *2 bp* GAcCAAGCCC(0.60)	High(3)
145 P2	148770727	148770746	19765	cAGCTTGTCT(0.63) *0 bp* AGACAgGCCC(0.60)	High(2)
145 P2	148770727	148770760	19765	cAGCTTGTCT(0.63) *14 bp* GGGCTTcaCC(0.41)	High(3)
145 P3	148779635	148779660	10767	GGGCcTGagC(0.46) *6 bp* AGGCAAGgCT(0.56)	High(4)
145 P4	148786552	148786574	3850	cAcCATGTTg(0.28) *3 bp* GGGCTgGTCT(0.32)	Medium(4)
145 P5	148788027	148788053	2375	AAACTTGagT(0.23) *7 bp* GAGCATaTTT(0.37)	Medium(3)
145 P6	148788310	148788344	2092	GGACTAGggg(0.23) *15 bp* GAGCTTcTTT(0.41)	Medium(4)
145 P7	148758872	148759369	31033	UCSC Genome Browser	

Primer ID	Conservation (mouse)
145 P1	Highly conserved in the Alignment block chr5:148764172-148764256
145 P2	Highly conserved in the Alignment block chr5:148770709-148770884
145 P2	Highly conserved in the Alignment block chr5:148770709-148770884
145 P3	Highly conserved in the Alignment block chr5:148779608-148779660
145 P4	Nearby CoVote promoter
145 P5	Nearby CoVote promoter
145 P6	Within CoVote promoter
145 P7	Highly conserved in the Alignment block chr5:148764172-148764256

Table 2. Reverse Phase Proteomic Array (RPPA) results after *miR-145* transfection.

MCF-7 (a)				MDA-MB-231 (a)			
Antibody id	**p-value (b)**	**FDR**	**Fold-change**	**Antibody id**	**p-value (b)**	**FDR**	**Fold-change**
ESR1	0.003	0.05	0.41	AKT.pS473	0.031	0.55	1.12
Rb.pS807	0.016	0.14	0.60	PDK1	0.042	0.57	1.12
IRS1.pS307	0.004	0.05	0.65	PDK1.pS241/PDK1	0.021	0.46	1.16
PTEN	0.005	0.05	0.69	PDK1.pS241	0.011	0.46	1.25
Rb	0.001	0.05	0.83	MEK	0.010	0.46	1.39
cyclinD1	0.007	0.07	0.85	Beta Catenin	0.035	0.55	1.66
ESR1.pS118	0.003	0.05	0.88				
mTOR	0.035	0.21	0.89				
JNK.pT183	0.001	0.05	1.14				
FKHRL1	0.004	0.05	1.19				
cJun.pS73	0.038	0.21	1.20				
Caspase7	0.034	0.21	1.21				
PDK1	0.000	0.05	1.21				
PDK1.pS241	0.028	0.20	1.23				
Bim	0.017	0.14	1.26				
JNK.pT183/JNK2	0.026	0.20	1.63				

Note:

a. The cells were collected after 36 hours from the transfection

b. The p-value was calculated using t-test with unequal variance between groups. *MiR-145* transfections (3 independent experiments) were compared to scrambled transfections (3 independent experiments) for each cell line. Only proteins for which the p values were lower than 0.05 are shown. Univariate two-sample *t*-test was used (BRB-ArrayTools Version: 3.6.1, http://linus.nci.nih.gov/BRB-ArrayTools.html)

c. FDR = False Discovery Rate

Table 3. Differentially expressed genes after miR-145 transfection in MCF7 cells by using Class Prediction method. Only genes differentially expressed at least two times in comparison with the scrambled oligo control are presented.

Parametric p-value	Geom mean of intensities in class CONTROL	Geom mean of intensities in class 145	Ratio of geom means CONTROL/145	Description	Gene symbol
7.60E-06	4.42	7433.50	**0.00060**	2'-5'-oligoadenylate synthetase 2, 69/71kDa	OAS2
0.0006686	23.45	24627.20	**0.00095**	interferon-induced protein with tetratricopeptide repeats 3	IFIT3
9.10E-06	5.13	5175.63	**0.00099**	interferon-induced protein 44-like	IFI44L
7.00E-06	6.03	4961.81	**0.00122**	interferon-induced protein with tetratricopeptide repeats 2	IFIT2
9.60E-06	5.25	3843.26	**0.00137**	interferon-induced protein 44	IFI44
1.60E-06	4.32	2985.54	**0.00145**	proteasome (prosome, macropain) subunit, beta type, 9 (large multifunctional peptidase 2)	PSMB9
7.67E-05	13.15	8756.29	**0.00150**	XIAP associated factor 1	XAF1
0.0001675	11.24	7061.37	**0.00159**	2'-5'-oligoadenylate synthetase-like	OASL
0.0002353	41.47	22870.82	**0.00181**	interferon-induced protein with tetratricopeptide repeats 2	IFIT2
3.93E-05	5.65	2805.04	**0.00201**	bone marrow stromal cell antigen 2	BST2
3.04E-05	5.19	2544.36	**0.00204**	chemokine (C-C motif) ligand 5	CCL5
6.99E-05	5.84	2823.35	**0.00207**	chemokine (C-C motif) ligand 5	CCL5
2.77E-05	6.88	3115.55	**0.00221**	chemokine (C-C motif) ligand 5	CCL5
5.72E-05	4.86	2053.13	**0.00237**	myxovirus (influenza virus) resistance 2 (mouse)	MX2
0.000188	14.16	5048.96	**0.00280**	hect domain and RLD 5	HERC5
4.68E-05	4.52	1505.27	**0.00300**	proteasome (prosome, macropain) subunit, beta type, 8 (large multifunctional peptidase 7)	PSMB8
4.72E-05	9.62	3001.63	**0.00320**	2'-5'-oligoadenylate synthetase 2, 69/71kDa	OAS2
0.0004408	5.18	1508.55	**0.00343**	interleukin 28A (interferon, lambda 2)	IL28A
7.48E-05	8.53	2269.98	**0.00376**	2'-5'-oligoadenylate synthetase 2, 69/71kDa	OAS2
0.0001856	5.81	1482.39	**0.00392**	tripartite motif-containing 22	TRIM22
3.43E-05	4.59	1000.00	**0.00459**	receptor (chemosensory) transporter protein 4	RTP4
0.0001468	5.17	1049.48	**0.00493**	interleukin 28A (interferon, lambda 2) /// interleukin 28B (interferon, lambda 3)	IL28A /// IL28B
0.0006633	9.83	1956.00	**0.00503**	tumor necrosis factor (ligand) superfamily, member 10	TNFSF10
0.0002874	4.20	800.14	**0.00524**	chemokine (C-X-C motif) ligand 10	CXCL10
7.40E-06	5.66	1068.70	**0.00530**	tumor necrosis factor (ligand) superfamily, member 10	TNFSF10
6.10E-05	5.36	884.71	**0.00606**	interleukin 29 (interferon, lambda 1)	IL29

0.0008592	99.15	16343.16	**0.00607**	cytidine monophosphate (UMP-CMP) kinase 2, mitochondrial	CMPK2
0.0001853	185.11	30479.13	**0.00607**	interferon, alpha-inducible protein 27	IFI27
0.0001136	5.65	905.75	**0.00624**	Interferon-induced protein 44	IFI44
1.24E-05	5.57	829.61	**0.00672**	chemokine (C-X-C motif) ligand 11	CXCL11
0.0003682	23.48	3448.17	**0.00681**	XIAP associated factor 1	XAF1
3.50E-06	5.07	743.69	**0.00682**	XIAP associated factor 1	XAF1
0.0001151	5.66	826.80	**0.00684**	sterile alpha motif domain containing 9-like	SAMD9L
5.35E-05	6.99	1011.12	**0.00692**	guanylate binding protein 3	GBP3
0.0001681	19.11	2719.94	**0.00703**	sterile alpha motif domain containing 9	SAMD9
9.29E-05	7.14	955.79	**0.00747**	hypothetical protein FLJ11286	FLJ11286
0.0002165	16.10	2116.05	**0.00761**	DEAD (Asp-Glu-Ala-Asp) box polypeptide 60-like	DDX60L
0.000183	71.52	9082.91	**0.00787**	ubiquitin-conjugating enzyme E2L 6	UBE2L6
0.0003449	6.30	755.15	**0.00834**	chemokine (C-X-C motif) ligand 11	CXCL11
0.0005568	6.10	708.40	**0.00861**	butyrophilin, subfamily 3, member A3 /// butyrophilin, subfamily 3, member A2	BTN3A2 /// BTN3A3
0.0005027	8.41	958.16	**0.00878**	tumor necrosis factor (ligand) superfamily, member 10	TNFSF10
0.0004585	6.39	725.64	**0.00881**	interferon, beta 1, fibroblast	IFNB1
7.80E-06	6.66	747.56	**0.00891**	guanylate binding protein 1, interferon-inducible, 67kDa	GBP1
0.0001461	310.36	34354.29	**0.00903**	interferon-induced protein with tetratricopeptide repeats 1	IFIT1
0.0003612	107.57	10997.95	**0.00978**	2',5'-oligoadenylate synthetase 1, 40/46kDa	OAS1
0.0001469	101.11	8280.79	**0.01221**	2',5'-oligoadenylate synthetase 1, 40/46kDa	OAS1
0.0003995	6.10	471.41	**0.01295**	complement factor B	CFB
2.05E-05	7.10	513.03	**0.01385**	apolipoprotein L, 3	APOL3
8.71E-05	14.85	956.80	**0.01552**	Transcribed locus	
8.66E-05	4.73	284.89	**0.01659**	NLR family, CARD domain containing 5	NLRC5
0.0007083	5.35	315.05	**0.01700**		
0.0002292	143.69	7775.70	**0.01848**	interferon stimulated exonuclease gene 20kDa	ISG20
0.0001796	3.70	197.00	**0.01878**	solute carrier family 15, member 3	SLC15A3
1.40E-05	186.09	9866.56	**0.01886**	interferon stimulated exonuclease gene 20kDa	ISG20
0.0002373	68.64	3634.04	**0.01889**	ubiquitin specific peptidase 18	USP18
9.09E-05	6.84	358.39	**0.01909**	CD74 molecule, major histocompatibility complex, class II invariant chain	CD74
0.0008459	80.86	4217.61	**0.01917**	interferon-induced protein 35	IFI35
0.0003491	6.91	346.42	**0.01994**		
0.0005639	3.21	155.71	**0.02064**	apolipoprotein L, 6	APOL6
0.0002101	5.62	271.35	**0.02071**	sterile alpha motif domain containing 9-like	SAMD9L
0.0005697	13.65	643.46	**0.02121**	SP100 nuclear antigen	SP100

0.0008512	3.94	183.74	**0.02144**	Transcribed locus	
3.60E-06	5.03	211.75	**0.02373**	lipase A, lysosomal acid, cholesterol esterase (Wolman disease)	LIPA
0.0005412	183.39	7668.03	**0.02392**	DEAD (Asp-Glu-Ala-Asp) box polypeptide 58	DDX58
0.0009418	5.01	202.17	**0.02476**	butyrophilin, subfamily 3, member A2	BTN3A2
0.0001011	489.75	19467.48	**0.02516**	interferon induced transmembrane protein 1 (9-27)	IFITM1
0.000334	10.08	393.73	**0.02560**	basic leucine zipper transcription factor, ATF-like 2	BATF2
0.0006988	6.37	237.15	**0.02686**	HLA complex P5	HCP5
0.0004541	62.30	2303.11	**0.02705**	DEAD (Asp-Glu-Ala-Asp) box polypeptide 58	DDX58
0.0006463	8.36	302.67	**0.02761**	butyrophilin, subfamily 3, member A3	BTN3A3
0.0001556	12.12	417.02	**0.02906**	SP110 nuclear body protein	SP110
0.000884	9.58	328.37	**0.02918**	apolipoprotein L, 1	APOL1
0.0005789	5.73	184.17	**0.03109**	PDZ domain containing 2	PDZD2
0.0008969	8.98	286.14	**0.03138**	butyrophilin, subfamily 3, member A3	BTN3A3
0.0006604	4.79	152.41	**0.03142**	interleukin 15	IL15
0.0005914	6.40	199.62	**0.03207**	myxovirus (influenza virus) resistance 1, interferon-inducible protein p78 (mouse)	MX1
0.0004362	7.23	220.71	**0.03278**	tripartite motif-containing 21	TRIM21
0.0001399	604.78	18272.78	**0.03310**	interferon induced transmembrane protein 1 (9-27)	IFITM1
0.000802	34.74	1033.94	**0.03360**	peroxisomal proliferator-activated receptor A interacting complex 285	PRIC285
5.01E-05	13.65	405.85	**0.03363**	hypothetical protein FLJ11286	FLJ11286
3.07E-05	106.13	3124.57	**0.03397**	poly (ADP-ribose) polymerase family, member 14	PARP14
0.0003454	16.34	465.04	**0.03513**	poly (ADP-ribose) polymerase family, member 10	PARP10
0.0004566	194.36	5395.74	**0.03602**	transporter 1, ATP-binding cassette, sub-family B (MDR/TAP)	TAP1
0.0001259	46.23	1240.41	**0.03727**	insulin-like growth factor binding protein 6	IGFBP6
6.38E-05	11.50	307.58	**0.03739**	2'-5'-oligoadenylate synthetase 3, 100kDa	OAS3
5.39E-05	234.49	6184.77	**0.03791**	poly (ADP-ribose) polymerase family, member 9	PARP9
0.0003265	8.19	215.39	**0.03804**	hypothetical gene supported by AK128882	LOC441108
0.0001135	357.40	8958.11	**0.03990**	major histocompatibility complex, class I, B	HLA-B
0.0001472	7.25	180.92	**0.04008**	apolipoprotein L, 6	APOL6
1.62E-05	353.86	8793.76	**0.04024**	interferon induced with helicase C domain 1	IFIH1
0.0005762	31.31	751.93	**0.04164**	interferon induced with helicase C domain 1	IFIH1
0.0003528	422.15	9755.79	**0.04327**	major histocompatibility complex, class I, B /// major histocompatibility complex, class I, C /// MHC class I polypeptide-related sequence A /// MHC class I polypeptide-related sequence B /// family with sequence similarity 20,	FAM20B /// HLA-B /// HLA-C /// MICA /// MICB /// XXbac-

				member B	BPG181B23.1
0.0001656	41.00	912.93	**0.04491**	transporter 2, ATP-binding cassette, sub-family B (MDR/TAP)	TAP2
0.0001801	92.93	2019.55	**0.04601**	hect domain and RLD 6	HERC6
0.000237	618.72	13126.64	**0.04713**	major histocompatibility complex, class I, B /// major histocompatibility complex, class I, C /// MHC class I polypeptide-related sequence A /// MHC class I polypeptide-related sequence B	HLA-B /// HLA-C /// MICA /// MICB /// XXbac-BPG181B23.1
0.0001375	423.75	8711.87	**0.04864**	2'-5'-oligoadenylate synthetase 3, 100kDa	OAS3
0.0002746	5.28	108.57	**0.04864**	major histocompatibility complex, class II, DR alpha	HLA-DRA
0.0003238	7.19	147.69	**0.04869**	dual adaptor of phosphotyrosine and 3-phosphoinositides	DAPP1
7.85E-05	96.57	1979.23	**0.04879**	poly (ADP-ribose) polymerase family, member 12	PARP12
0.00044	24.53	495.48	**0.04952**	tumor necrosis factor, alpha-induced protein 3	TNFAIP3
7.91E-05	8.82	172.34	**0.05115**	plasminogen activator, urokinase receptor	PLAUR
4.58E-05	6.24	121.02	**0.05156**	endoplasmic reticulum aminopeptidase 2	ERAP2
0.0001219	6.97	134.29	**0.05186**	C-type lectin domain family 7, member A	CLEC7A
2.58E-05	32.76	614.38	**0.05333**	promyelocytic leukemia	PML
0.0006582	5.15	94.02	**0.05477**	major histocompatibility complex, class II, DP alpha 1	HLA-DPA1
3.60E-05	4.93	86.80	**0.05676**	Z-DNA binding protein 1	ZBP1
0.0003094	43.79	769.70	**0.05689**	zinc finger CCCH-type, antiviral 1	ZC3HAV1
0.0001342	139.24	2279.32	**0.06109**	SP110 nuclear body protein	SP110
7.10E-05	826.39	13505.02	**0.06119**	interferon, alpha-inducible protein 6	IFI6
0.0006802	323.61	5228.35	**0.06190**	Transcribed locus	
0.0001426	40.00	635.92	**0.06291**	ring finger protein 213	RNF213
7.00E-04	7.36	116.70	**0.06310**	complement component 1, r subcomponent	C1R
0.0004818	10.41	164.07	**0.06344**	baculoviral IAP repeat-containing 3	BIRC3
0.0008824	17.79	279.16	**0.06373**	guanine nucleotide binding protein (G protein), beta polypeptide 4	GNB4
0.0002251	34.31	526.96	**0.06511**	HRAS-like suppressor 2	HRASLS2
0.0005839	556.54	8515.36	**0.06536**	Transcribed locus	
6.12E-05	428.85	6553.86	**0.06543**	lectin, galactoside-binding, soluble, 3 binding protein	LGALS3BP
2.56E-05	241.39	3675.52	**0.06567**	major histocompatibility complex, class I, F	HLA-F
0.0004231	13.74	205.22	**0.06693**	Full length insert cDNA clone YR04D03	
0.0001856	17.47	252.12	**0.06930**	insulin-like growth factor binding protein 3	IGFBP3
2.84E-05	517.69	7464.40	**0.06936**	phospholipid scramblase 1	PLSCR1

0.0004116	6.61	94.93	**0.06966**	sema domain, transmembrane domain (TM), and cytoplasmic domain, (semaphorin) 6D	SEMA6D
0.0007967	33.68	483.48	**0.06967**	optineurin	OPTN
0.00051	4.34	61.89	**0.07016**	plexin A2	PLXNA2
0.0004653	172.82	2424.53	**0.07128**	SP100 nuclear antigen	SP100
0.0002396	170.64	2384.93	**0.07155**	SP110 nuclear body protein	SP110
0.0005122	21.84	300.89	**0.07257**	betacellulin	BTC
0.0001094	582.79	7955.61	**0.07326**	signal transducer and activator of transcription 1, 91kDa	STAT1
3.27E-05	1428.04	19315.74	**0.07393**	phospholipid scramblase 1	PLSCR1
6.82E-05	204.14	2718.23	**0.07510**	major histocompatibility complex, class I, F	HLA-F
9.91E-05	809.70	10711.22	**0.07559**	N-myc (and STAT) interactor	NMI
2.20E-06	6.00	79.08	**0.07582**	Transcribed locus	
0.0009548	1102.86	14543.48	**0.07583**	major histocompatibility complex, class I, A	HLA-A
0.0002111	251.39	3282.48	**0.07658**	nuclear receptor coactivator 7	NCOA7
0.0001047	144.45	1830.87	**0.07889**	SP100 nuclear antigen	SP100
0.0002709	8.74	108.86	**0.08030**	CDNA FLJ46701 fis, clone TRACH3014063	
6.21E-05	14.78	180.43	**0.08194**	SP110 nuclear body protein	SP110
3.18E-05	191.27	2325.54	**0.08225**	major histocompatibility complex, class I, J (pseudogene)	HLA-J
0.0002988	27.97	340.09	**0.08225**	Viral DNA polymerase-transactivated protein 6	LOC26010
0.0004242	9.81	117.66	**0.08334**	betacellulin	BTC
4.78E-05	162.89	1923.29	**0.08469**	interferon-induced protein with tetratricopeptide repeats 5	IFIT5
0.0001145	189.22	2211.25	**0.08557**	optineurin	OPTN
0.000821	5.98	68.47	**0.08730**	ring finger protein 213	RNF213
0.0004719	1356.41	15247.07	**0.08896**	major histocompatibility complex, class I, C	HLA-C
7.34E-05	5.63	59.44	**0.09468**	tripartite motif-containing 38	TRIM38
0.0002043	1060.95	11167.82	**0.09500**	major histocompatibility complex, class I, B /// major histocompatibility complex, class I, C /// MHC class I polypeptide-related sequence A /// MHC class I polypeptide-related sequence B	HLA-B /// HLA-C /// MICA /// MICB /// XXbac-BPG181B23.1
0.0003053	125.62	1321.84	**0.09503**	interferon regulatory factor 7	IRF7
0.000252	471.27	4955.82	**0.09509**	interferon-induced protein with tetratricopeptide repeats 5	IFIT5
0.0006451	18.41	191.13	**0.09634**	plasminogen activator, urokinase receptor	PLAUR
5.44E-05	7.45	76.30	**0.09765**	Transcribed locus	
0.0006884	33.46	338.20	**0.09893**	suppressor of cytokine signaling 1	SOCS1
0.0001035	1711.98	16781.73	**0.10201**	major histocompatibility complex, class I, C	HLA-C

0.0006519	11.65	111.87	**0.10418**	tripartite motif-containing 34 /// tripartite motif-containing 6 /// TRIM6-TRIM34	TRIM34 /// TRIM6 /// TRIM6-TRIM34
3.80E-06	811.57	7683.90	**0.10562**	major histocompatibility complex, class I, A	HLA-A
0.0002243	3.55	33.48	**0.10617**	ATPase, H+ transporting, lysosomal 42kDa, V1 subunit C2	ATP6V1C2
0.0001858	222.36	1989.88	**0.11175**	ring finger protein 213	RNF213
0.0003134	353.06	3009.90	**0.11730**	signal transducer and activator of transcription 1, 91kDa	STAT1
0.0003185	169.70	1437.87	**0.11802**	ring finger protein 213	RNF213
0.0001384	38.16	323.16	**0.11810**	hematopoietic SH2 domain containing	HSH2D
0.0005631	11.46	96.78	**0.11843**	Mitogen-activated protein kinase kinase kinase 8 /// CDNA clone IMAGE:4689481	MAP3K8
0.0002861	49.93	406.39	**0.12285**	TAP binding protein-like	TAPBPL
7.10E-06	552.35	4470.26	**0.12356**	signal transducer and activator of transcription 1, 91kDa	STAT1
0.0003063	342.04	2758.40	**0.12400**	major histocompatibility complex, class I, G	HLA-G
0.0002481	646.37	5138.97	**0.12578**	major histocompatibility complex, class I, G	HLA-G
0.000894	49.13	390.11	**0.12594**	chromosome 14 open reading frame 83	C14orf83
0.0003366	348.31	2734.13	**0.12739**	zinc finger, NFX1-type containing 1	ZNFX1
0.000197	395.90	3093.32	**0.12799**	proteasome (prosome, macropain) subunit, beta type, 10	PSMB10
0.0002017	84.94	662.14	**0.12828**	tripartite motif-containing 5	TRIM5
0.0001396	678.50	5112.61	**0.13271**		
0.0007318	34.50	259.00	**0.13321**	pleckstrin homology-like domain, family B, member 2	PHLDB2
0.0001534	167.16	1229.93	**0.13591**	major histocompatibility complex, class I, E	HLA-E
0.0003412	6.46	46.94	**0.13768**	viral DNA polymerase-transactivated protein 6	LOC26010
2.47E-05	842.82	6112.57	**0.13788**	tryptophanyl-tRNA synthetase	WARS
0.0004005	87.26	632.77	**0.13791**	major histocompatibility complex, class I, G	HLA-G
1.40E-06	6982.38	50002.10	**0.13964**	ISG15 ubiquitin-like modifier	ISG15
0.000265	121.11	858.75	**0.14103**	mixed lineage kinase domain-like	MLKL
0.0007893	52.21	370.15	**0.14104**	calpain 8 /// similar to calpain 8	CAPN8 /// LOC644151
0.0001874	97.01	686.19	**0.14138**	aquaporin 3 (Gill blood group)	AQP3
8.68E-05	810.54	5610.73	**0.14446**	tryptophanyl-tRNA synthetase	WARS
0.0003264	437.98	3008.20	**0.14560**	signal transducer and activator of transcription 2, 113kDa	STAT2
0.0001967	139.71	958.62	**0.14574**	carcinoembryonic antigen-related cell adhesion molecule 5	CEACAM5
0.0005108	1225.55	8364.90	**0.14651**	major histocompatibility complex, class I, E	HLA-E

0.0006049	67.37	455.11	**0.14802**	TAP binding protein-like	TAPBPL
6.08E-05	521.95	3478.10	**0.15007**	deltex 3-like (Drosophila)	DTX3L
0.0003923	4.19	27.84	**0.15039**	promyelocytic leukemia /// hypothetical protein LOC161527	LOC161527 /// PML
8.90E-05	2324.59	15425.96	**0.15069**	interferon induced transmembrane protein 2 (1-8D)	IFITM2
0.0003847	562.51	3709.16	**0.15165**	signal transducer and activator of transcription 1, 91kDa	STAT1
1.00E-05	95.28	627.01	**0.15196**	endoplasmic reticulum aminopeptidase 1	ERAP1
0.0009172	396.24	2604.61	**0.15213**	tripartite motif-containing 14	TRIM14
4.61E-05	65.31	427.44	**0.15279**	cytochrome P450, family 2, subfamily J, polypeptide 2	CYP2J2
2.20E-05	145.57	929.94	**0.15653**	proline rich 15	PRR15
4.19E-05	553.95	3498.53	**0.15834**	interferon regulatory factor 9	IRF9
0.0001161	169.21	1008.59	**0.16777**	endoplasmic reticulum aminopeptidase 1	ERAP1
0.0002703	304.70	1801.46	**0.16914**	tudor domain containing 7	TDRD7
0.0002066	3813.81	22313.41	**0.17092**	interferon induced transmembrane protein 3 (1-8U)	IFITM3
0.0008091	456.62	2646.30	**0.17255**	major histocompatibility complex, class I, E	HLA-E
8.26E-05	1637.99	9379.41	**0.17464**	aquaporin 3 (Gill blood group)	AQP3
0.0006051	6.28	35.48	**0.17694**	PCTAIRE protein kinase 3	PCTK3
0.0007252	553.72	3087.94	**0.17932**	PHD finger protein 11	PHF11
4.89E-05	173.53	965.82	**0.17967**	negative regulator of ubiquitin-like proteins 1	NUB1
0.0002536	24.82	137.35	**0.18073**	ATP-binding cassette, sub-family D (ALD), member 1	ABCD1
3.46E-05	2892.77	15957.72	**0.18128**	metallothionein 2A	MT2A
0.0008812	58.07	313.66	**0.18514**	interferon regulatory factor 2	IRF2
0.0002979	146.80	789.37	**0.18597**	phorbol-12-myristate-13-acetate-induced protein 1	PMAIP1
0.0009901	175.59	941.20	**0.18656**	solute carrier family 25, member 28	SLC25A28
0.0002465	160.37	843.94	**0.19002**	chemokine (C-X-C motif) ligand 16	CXCL16
0.0007372	1047.20	5494.27	**0.19060**	signal transducer and activator of transcription 1, 91kDa	STAT1
0.0001529	16.93	87.93	**0.19257**	Transcribed locus	
0.0005212	1089.25	5645.14	**0.19295**	metallothionein 1X	MT1X
0.000294	2052.33	10496.82	**0.19552**	polyribonucleotide nucleotidyltransferase 1	PNPT1
2.07E-05	10.04	50.74	**0.19778**		
7.28E-05	1256.99	6331.08	**0.19854**	S100 calcium binding protein P	S100P
0.0008254	614.47	3044.47	**0.20183**	metallothionein 1 pseudogene 2	MT1P2
0.0008212	562.21	2765.99	**0.20326**	family with sequence similarity 46, member A	FAM46A

0.0007169	389.22	1869.48	**0.20820**	phorbol-12-myristate-13-acetate-induced protein 1	PMAIP1
0.0002661	3503.06	16753.90	**0.20909**	leucine aminopeptidase 3	LAP3
0.0005557	201.21	955.87	**0.21050**	family with sequence similarity 46, member A	FAM46A
0.0002162	93.87	442.58	**0.21210**	endothelin 1	EDN1
0.0001582	63.28	298.09	**0.21229**	Partial mRNA; ID EE2-8E	
0.0007858	485.09	2266.13	**0.21406**	metallothionein 1H	MT1H
0.000822	153.37	716.46	**0.21407**	tripartite motif-containing 56	TRIM56
0.000305	358.34	1655.84	**0.21641**	tumor necrosis factor receptor superfamily, member 11b (osteoprotegerin)	TNFRSF11B
0.0002641	118.15	533.21	**0.22158**	leucine rich repeat containing 50	LRRC50
0.0002572	163.63	718.41	**0.22777**	neural precursor cell expressed, developmentally down-regulated 9	NEDD9
0.0005667	7.53	32.86	**0.22906**	Transcribed locus	
0.000442	679.03	2911.31	**0.23324**	eukaryotic translation initiation factor 2-alpha kinase 2	EIF2AK2
6.09E-05	8.50	35.98	**0.23620**	peroxisomal proliferator-activated receptor A interacting complex 285	PRIC285
3.60E-06	54.19	226.19	**0.23955**	chromosome 11 open reading frame 17 /// NUAK family, SNF1-like kinase, 2	C11orf17 /// NUAK2
0.0009328	10.17	42.23	**0.24075**	major histocompatibility complex, class II, DP alpha 1	HLA-DPA1
0.0003283	169.99	704.87	**0.24116**	endothelin 1	EDN1
3.93E-05	91.32	378.19	**0.24146**	endothelial PAS domain protein 1	EPAS1
0.000103	148.60	606.49	**0.24501**	opioid growth factor receptor	OGFR
0.0004809	12.47	50.06	**0.24907**	negative regulator of ubiquitin-like proteins 1	NUB1
0.0008934	47.58	190.32	**0.25001**	guanylate binding protein 2, interferon-inducible	GBP2
0.0002273	398.57	1569.84	**0.25389**	midkine (neurite growth-promoting factor 2)	MDK
4.98E-05	199.49	777.87	**0.25646**	opioid growth factor receptor	OGFR
0.0008878	2633.02	10075.45	**0.26133**	nuclear factor of kappa light polypeptide gene enhancer in B-cells inhibitor, alpha	NFKBIA
0.0003297	282.86	1064.97	**0.26560**	polycomb group ring finger 5	PCGF5
0.0003119	27.11	101.97	**0.26587**	claudin 23	CLDN23
0.0009833	74.06	276.49	**0.26784**	claudin 1	CLDN1
0.0001659	95.25	354.15	**0.26895**	runt-related transcription factor 2	RUNX2
0.0007779	335.46	1231.63	**0.27237**	NEDD4 binding protein 1	N4BP1
0.0006319	393.68	1429.03	**0.27549**	nuclear factor of kappa light polypeptide gene enhancer in B-cells inhibitor, zeta	NFKBIZ
0.0003494	205.47	744.62	**0.27594**	B-cell CLL/lymphoma 6 (zinc finger protein 51)	BCL6
4.45E-05	33.00	118.20	**0.27919**	G protein-coupled receptor 115	GPR115

0.000194	1056.99	3744.80	**0.28226**	DNA-damage-inducible transcript 4	DDIT4
0.0003278	11375.30	39816.66	**0.28569**	beta-2-microglobulin	B2M
0.0004951	375.93	1303.65	**0.28837**	carcinoembryonic antigen-related cell adhesion molecule 6 (non-specific cross reacting antigen)	CEACAM6
0.0004003	115.44	399.29	**0.28912**	tripartite motif-containing 25	TRIM25
0.0009159	34.06	115.89	**0.29386**	tripartite motif-containing 47	TRIM47
0.0002739	176.43	599.68	**0.29420**	polycomb group ring finger 5	PCGF5
0.000117	1489.89	5047.60	**0.29517**	lymphocyte antigen 6 complex, locus E	LY6E
0.0009564	116.70	393.31	**0.29672**	male sterility domain containing 1	MLSTD1
0.0001706	1151.44	3874.11	**0.29721**	phosphoinositide-3-kinase, regulatory subunit 2 (beta) /// interferon, gamma-inducible protein 30	IFI30 /// PIK3R2
7.80E-06	85.80	287.12	**0.29881**	three prime repair exonuclease 1 /// ATR interacting protein	ATRIP /// TREX1
0.0003923	14.10	46.98	**0.30010**	SRY (sex determining region Y)-box 9 (campomelic dysplasia, autosomal sex-reversal)	SOX9
0.0009785	218.94	717.11	**0.30530**	zinc finger, CCHC domain containing 2	ZCCHC2
0.0001527	711.13	2314.21	**0.30729**	acyl-CoA synthetase long-chain family member 1	ACSL1
0.0003248	2200.36	7123.16	**0.30890**	ELOVL family member 7, elongation of long chain fatty acids (yeast)	ELOVL7
0.0008196	175.41	564.48	**0.31074**	OTU domain containing 1	OTUD1
4.75E-05	280.81	887.07	**0.31656**	UDP-Gal:betaGlcNAc beta 1,4- galactosyltransferase, polypeptide 5	B4GALT5
0.0004258	185.31	584.55	**0.31702**	MAX dimerization protein 1	MXD1
0.0005821	712.08	2240.08	**0.31788**	eukaryotic translation initiation factor 2-alpha kinase 2	EIF2AK2
0.0006556	644.93	2026.51	**0.31825**		
0.0001263	138.54	429.82	**0.32233**	CD47 molecule	CD47
0.0001357	1208.92	3742.20	**0.32305**	ring finger protein 149	RNF149
0.000441	41.22	127.58	**0.32313**	ring finger protein 19B	RNF19B
0.0002643	488.84	1509.97	**0.32374**	zinc finger CCCH-type, antiviral 1	ZC3HAV1
2.66E-05	2844.87	8726.27	**0.32601**	proteasome (prosome, macropain) activator subunit 1 (PA28 alpha)	PSME1
5.79E-05	49.34	151.27	**0.32619**	Homo sapiens, clone IMAGE:5218412, mRNA	
0.0006686	54.55	166.19	**0.32826**	growth factor receptor-bound protein 10	GRB10
0.0003247	145.09	439.50	**0.33013**	GATA binding protein 6	GATA6
0.0009577	705.25	2106.96	**0.33472**	zinc finger protein 36, C3H type-like 2	ZFP36L2
0.0006201	191.60	560.55	**0.34181**	caspase 8, apoptosis-related cysteine peptidase	CASP8

0.0002877	802.41	2333.71	**0.34383**	argininosuccinate synthetase 1	ASS1
0.0006269	6.25	17.97	**0.34759**		
2.57E-05	380.06	1091.29	**0.34827**	Kruppel-like factor 3 (basic)	KLF3
0.0006916	757.62	2161.38	**0.35052**	shisa homolog 5 (Xenopus laevis)	SHISA5
1.31E-05	813.47	2311.28	**0.35196**	TAP binding protein (tapasin)	TAPBP
0.0001558	364.17	1031.76	**0.35296**	ubiquitin specific peptidase 42	USP42
0.0005033	73.76	207.04	**0.35626**	solute carrier organic anion transporter family, member 3A1	SLCO3A1
0.0006933	174.04	486.39	**0.35783**	Transcribed locus	
0.0005093	276.60	772.97	**0.35784**	dihydropyrimidine dehydrogenase	DPYD
2.70E-06	25.29	70.00	**0.36133**	protein phosphatase 1, regulatory (inhibitor) subunit 15A	PPP1R15A
0.0001659	435.19	1180.66	**0.36860**	BCL2-like 11 (apoptosis facilitator)	BCL2L11
0.0002127	866.13	2338.98	**0.37030**	stomatin	STOM
0.0009506	47.27	126.99	**0.37221**	Fas (TNF receptor superfamily, member 6)	FAS
0.0005954	80.02	212.77	**0.37608**	PDZ domain containing 1	PDZK1
0.0002617	785.28	2077.31	**0.37803**	calpastatin	CAST
4.29E-05	239.43	633.22	**0.37812**	2',3'-cyclic nucleotide 3' phosphodiesterase	CNP
0.0002215	187.53	493.78	**0.37978**	WNT1 inducible signaling pathway protein 2	WISP2
0.0004058	69.64	183.23	**0.38007**	protein phosphatase 1, regulatory (inhibitor) subunit 15A	PPP1R15A
0.0002078	90.87	238.47	**0.38105**	CD47 molecule	CD47
0.0005111	316.73	824.32	**0.38423**	phosphatidic acid phosphatase type 2A	PPAP2A
0.0002732	174.18	453.23	**0.38432**	lipin 1	LPIN1
0.0008676	632.91	1640.52	**0.38580**	zinc finger CCCH-type, antiviral 1	ZC3HAV1
0.0005783	2436.81	6304.71	**0.38651**	chemokine (C-X-C motif) receptor 7	CXCR7
0.000695	3258.40	8424.00	**0.38680**	chromatin modifying protein 5	CHMP5
8.92E-05	1107.69	2861.50	**0.38710**	inhibitor of DNA binding 3, dominant negative helix-loop-helix protein	ID3
0.0001103	2454.05	6334.14	**0.38743**	chromatin modifying protein 5	CHMP5
0.0008828	251.19	645.24	**0.38930**	tripartite motif-containing 26	TRIM26
0.0007107	1295.16	3318.42	**0.39029**	RanBP-type and C3HC4-type zinc finger containing 1	RBCK1
0.0008177	19.19	48.47	**0.39581**	chromosome 17 open reading frame 68	C17orf68
0.0003597	195.10	492.63	**0.39603**	Transcribed locus	
0.0005771	1164.82	2930.35	**0.39750**	calpastatin	CAST
0.0006862	84.99	210.75	**0.40328**	ring finger protein 43	RNF43
0.0005353	6454.15	15955.45	**0.40451**	CD47 molecule	CD47
0.0002547	333.64	816.10	**0.40882**	BCL2-like 11 (apoptosis facilitator)	BCL2L11
0.0001717	631.30	1532.01	**0.41207**	EH-domain containing 4	EHD4
0.0007668	1478.52	3560.17	**0.41529**	tripartite motif-containing 25	TRIM25

3.50E-06	378.32	910.01	**0.41573**	interleukin 6 signal transducer (gp130, oncostatin M receptor)	IL6ST
5.41E-05	219.25	520.39	**0.42132**	cathepsin C	CTSC
0.0001814	104.03	246.89	**0.42136**	coiled-coil domain containing 64	CCDC64
0.00012	3154.20	7461.72	**0.42272**	H2B histone family, member S	H2BFS
0.0004065	1723.27	4058.93	**0.42456**	nicotinamide phosphoribosyltransferase	NAMPT
0.0002244	424.97	994.67	**0.42725**	tumor necrosis factor receptor superfamily, member 21	TNFRSF21
0.0003057	232.30	541.60	**0.42891**	WAS protein homology region 2 domain containing 1	WHDC1
0.0003611	2639.95	6153.31	**0.42903**	Kruppel-like factor 4 (gut)	KLF4
0.000799	194.46	452.32	**0.42991**	ubiquitously transcribed tetratricopeptide repeat, X chromosome	UTX
9.70E-05	125.14	290.48	**0.43081**	protein associated with topoisomerase II homolog 1 (yeast)	PATL1
0.0007756	5845.42	13565.60	**0.43090**	CCAAT/enhancer binding protein (C/EBP), beta	CEBPB
0.0003743	822.52	1900.08	**0.43289**	histone cluster 1, H2bg /// histone cluster 1, H2bf /// histone cluster 1, H2be /// histone cluster 1, H2bi /// histone cluster 1, H2bc	HIST1H2BC /// HIST1H2BE /// HIST1H2BF /// HIST1H2BG /// HIST1H2BI
0.0009513	25.84	59.64	**0.43334**		
0.0004806	81.04	185.70	**0.43642**	transmembrane protein 51	TMEM51
0.0002683	8358.48	19140.72	**0.43669**	histone cluster 1, H2bk	HIST1H2BK
8.76E-05	1175.04	2686.08	**0.43745**	SAR1 gene homolog A (S. cerevisiae)	SAR1A
0.0002385	403.27	920.12	**0.43828**	DNA cross-link repair 1C (PSO2 homolog, S. cerevisiae)	DCLRE1C
1.36E-05	6518.25	14806.46	**0.44023**	metastasis associated lung adenocarcinoma transcript 1 (non-protein coding)	MALAT1
0.0003468	697.75	1582.15	**0.44101**	nicotinamide phosphoribosyltransferase	NAMPT
2.05E-05	169.45	383.88	**0.44142**	acid phosphatase 2, lysosomal	ACP2
0.0004032	54.67	123.79	**0.44162**	Src homology 2 domain containing adaptor protein B	SHB
0.0009688	65.15	147.09	**0.44290**	ubiquitin specific peptidase 42	USP42
0.0002163	417.92	941.80	**0.44374**	ovo-like 1(Drosophila)	OVOL1
0.0009655	714.75	1607.43	**0.44466**	ribosome binding protein 1 homolog 180kDa (dog)	RRBP1
0.0001776	457.81	1020.34	**0.44868**	lectin, galactoside-binding, soluble, 8 (galectin 8)	LGALS8
0.0004606	730.08	1618.57	**0.45107**	HIR histone cell cycle regulation defective homolog A (S. cerevisiae)	HIRA
0.0003848	52.69	116.65	**0.45168**	ectodermal-neural cortex (with BTB-like domain)	ENC1
0.0006403	739.02	1631.88	**0.45286**	KIAA1033	KIAA1033
0.0007433	1161.66	2548.94	**0.45574**	Transcribed locus, strongly similar to XP_531236.1 PREDICTED: hypothetical protein [Pan troglodytes]	

0.0005202	272.55	597.04	**0.45651**	dynein, cytoplasmic 1, heavy chain 1	DYNC1H1
0.0005621	713.49	1552.38	**0.45961**	KIAA1033	KIAA1033
0.0005771	1176.14	2553.92	**0.46052**	adhesion molecule with Ig-like domain 2	AMIGO2
0.000586	59.60	129.32	**0.46091**	chromosome 21 open reading frame 91	C21orf91
0.000882	8.47	18.14	**0.46672**	similar to WDNM1-like protein	LOC645638
0.000955	179.82	85.41	**2.10538**	trinucleotide repeat containing 6B	TNRC6B
0.0005292	74.05	34.31	**2.15839**	pleckstrin homology domain containing, family B (evectins) member 1	PLEKHB1
0.0006822	3527.49	1624.56	**2.17136**	metastasis suppressor 1	MTSS1
0.0002322	1904.41	871.95	**2.18407**	kinesin family member 14	KIF14
0.0002874	3999.30	1828.10	**2.18768**	pituitary tumor-transforming 1	PTTG1
0.0009425	656.60	297.81	**2.20473**	CDNA FLJ38388 fis, clone FEBRA2004485	
0.0001797	815.69	369.08	**2.21009**	sortilin 1	SORT1
0.000619	1008.52	456.02	**2.21156**	mindbomb homolog 1 (Drosophila)	MIB1
0.0007878	2876.55	1300.48	**2.21192**	integrin, alpha E (antigen CD103, human mucosal lymphocyte antigen 1; alpha polypeptide)	ITGAE
0.0005497	136.98	61.87	**2.21419**	Ts translation elongation factor, mitochondrial	TSFM
0.0005968	881.34	397.80	**2.21555**	HBS1-like (S. cerevisiae)	HBS1L
0.0007832	602.69	271.89	**2.21665**	ataxin 1	ATXN1
0.0009379	621.04	279.20	**2.22439**	vesicle transport through interaction with t-SNAREs homolog 1B (yeast)	VTI1B
0.0008403	2724.51	1222.24	**2.22911**	protein tyrosine phosphatase type IVA, member 2	PTP4A2
0.0007475	2472.17	1104.81	**2.23764**	hCG1815491	hCG_1815491
0.0005307	668.54	298.61	**2.23884**	H2A histone family, member V	H2AFV
0.0007782	655.24	292.58	**2.23955**	HBV preS1-transactivated protein 4	PS1TP4
0.0007587	234.75	104.62	**2.24377**	anthrax toxin receptor 1	ANTXR1
8.09E-05	1079.72	481.19	**2.24384**	doublecortin domain containing 2	DCDC2
0.0003458	3270.39	1456.27	**2.24573**	ribosomal protein L22	RPL22
4.10E-05	854.51	379.85	**2.24958**	IMP1 inner mitochondrial membrane peptidase-like (S. cerevisiae)	IMMP1L
0.0004087	3842.99	1707.47	**2.25070**	hyaluronan-mediated motility receptor (RHAMM)	HMMR
0.0001149	1163.55	515.74	**2.25608**	prenylcysteine oxidase 1	PCYOX1
0.000251	208.57	92.44	**2.25629**	pallidin homolog (mouse)	PLDN
0.0007916	114.71	50.81	**2.25766**		
0.0003073	419.13	185.23	**2.26271**	transmembrane protein 183A	TMEM183A
0.0003525	401.73	177.14	**2.26785**	DIP2 disco-interacting protein 2 homolog C (Drosophila)	DIP2C
6.70E-06	28.84	12.69	**2.27181**	Transcribed locus	

2.47E-05	9687.38	4260.99	**2.27350**	nuclear casein kinase and cyclin-dependent kinase substrate 1	NUCKS1
0.0001803	259.06	113.59	**2.28069**	amyotrophic lateral sclerosis 2 (juvenile) chromosome region, candidate 13	ALS2CR13
0.0006929	137.11	60.06	**2.28300**	CDNA clone IMAGE:5313062	
0.0008814	158.27	69.19	**2.28748**	leptin receptor	LEPR
0.0005918	112.08	48.76	**2.29829**	Transcribed locus	
2.63E-05	310.17	133.22	**2.32833**	M-phase phosphoprotein 9	MPHOSPH9
0.0003843	1123.31	474.73	**2.36620**	sterile alpha motif and leucine zipper containing kinase AZK	ZAK
4.80E-05	2331.27	981.02	**2.37637**	kinesin family member 20A	KIF20A
0.0007608	2732.66	1148.16	**2.38004**	Homo sapiens, Similar to likely ortholog of yeast ARV1, clone IMAGE:3460560, mRNA	
0.0001641	212.77	88.74	**2.39782**	chitinase 3-like 2	CHI3L2
0.0002328	482.03	200.47	**2.40445**	ubiquitination factor E4B (UFD2 homolog, yeast)	UBE4B
0.0008995	313.66	129.99	**2.41294**	coiled-coil domain containing 74A /// coiled-coil domain containing 74B	CCDC74A /// CCDC74B
0.0005756	707.74	293.00	**2.41551**	SERPINE1 mRNA binding protein 1	SERBP1
0.000391	2370.73	979.93	**2.41929**	mesoderm specific transcript homolog (mouse)	MEST
0.000299	179.10	73.82	**2.42608**	septin 11	12-Sep
0.000283	2175.76	893.16	**2.43603**	Growth arrest-specific 2 like 3	GAS2L3
0.0009384	181.53	74.50	**2.43677**	hypothetical protein LOC203547	LOC203547
0.0007565	71.37	29.05	**2.45692**	phosphorylase kinase, beta	PHKB
0.0002413	292.65	118.77	**2.46398**	Transcribed locus	
0.0008124	748.86	302.40	**2.47644**	prenylcysteine oxidase 1	PCYOX1
0.0008165	3148.47	1270.37	**2.47838**	helicase, lymphoid-specific	HELLS
0.0009149	291.13	117.21	**2.48382**	coactosin-like 1 (Dictyostelium)	COTL1
0.0005144	346.10	139.24	**2.48559**	sterile alpha motif and leucine zipper containing kinase AZK	ZAK
0.0007054	187.80	75.51	**2.48708**	CDNA clone IMAGE:4157286	
0.000411	1205.75	484.51	**2.48860**	transmembrane protein 64	TMEM64
0.000449	785.17	313.10	**2.50776**	Hypothetical protein LOC143381	LOC143381
0.000872	1790.36	712.26	**2.51363**	hyaluronan-mediated motility receptor (RHAMM)	HMMR
0.0005345	383.16	152.38	**2.51452**	CDNA FLJ31919 fis, clone NT2RP7004964	
0.0009989	69.05	26.89	**2.56815**	zinc fingers and homeoboxes 3	ZHX3
0.0004951	130.09	50.47	**2.57769**	PHD finger protein 17	PHF17
0.0007402	585.03	226.51	**2.58279**	Eukaryotic translation initiation factor 2C, 2	EIF2C2
0.0007321	1185.94	457.58	**2.59175**	CDNA clone IMAGE:3346313	
4.05E-05	16309.64	6275.42	**2.59897**	Transcribed locus	

0.0005771	741.37	280.51	**2.64291**	CDNA: FLJ21763 fis, clone COLF6967	
0.0008353	317.46	118.71	**2.67428**	myelin expression factor 2	MYEF2
0.0009725	1199.84	447.02	**2.68409**	KIAA0152	KIAA0152
0.0004418	1766.32	657.10	**2.68806**	Protein kinase, cAMP-dependent, regulatory, type II, alpha	PRKAR2A
0.0007336	2140.96	792.88	**2.70023**	limb region 1 homolog (mouse)	LMBR1
8.92E-05	404.25	149.19	**2.70958**	CDNA FLJ32526 fis, clone SMINT2000073	
0.0007144	1571.04	578.75	**2.71454**	DEP domain containing 1	DEPDC1
0.0005023	718.10	263.83	**2.72184**	trafficking protein, kinesin binding 2	TRAK2
0.0005593	177.24	65.08	**2.72324**	KIAA1797	KIAA1797
0.0006755	974.50	356.49	**2.73362**	prostate transmembrane protein, androgen induced 1	PMEPA1
0.0002667	113.65	41.48	**2.73962**	MRNA; cDNA DKFZp686K0394 (from clone DKFZp686K0394)	
0.0001005	76.32	27.77	**2.74824**	CDNA clone IMAGE:5261213	
0.0006308	751.00	271.58	**2.76530**	solute carrier family 38, member 1	SLC38A1
0.0003361	403.05	145.33	**2.77324**	CDNA FLJ39067 fis, clone NT2RP7014910 /// CDNA FLJ38048 fis, clone CTONG2014264	
0.000687	1181.83	425.91	**2.77486**	peptidylprolyl isomerase A (cyclophilin A)	PPIA
0.0006279	346.45	122.83	**2.82068**	angiomotin like 1	AMOTL1
0.0008412	1640.20	581.18	**2.82218**	H2A histone family, member V	H2AFV
0.000773	260.75	90.38	**2.88514**	adducin 3 (gamma)	ADD3
6.39E-05	1745.72	599.66	**2.91120**	DEP domain containing 1	DEPDC1
0.0002787	989.78	335.80	**2.94749**	atlastin 3	ATL3
0.0009596	137.84	46.55	**2.96078**	sortilin 1	SORT1
0.0004955	3718.27	1249.04	**2.97692**	Transcribed locus	
0.0007639	1308.06	438.88	**2.98045**	high-mobility group box 3	HMGB3
0.0002931	38.17	12.80	**2.98146**	cadherin 18, type 2	CDH18
0.0005742	672.72	224.50	**2.99649**	CKLF-like MARVEL transmembrane domain containing 4	CMTM4
0.0003936	276.76	88.79	**3.11696**	CDNA: FLJ22515 fis, clone HRC12122, highly similar to AF052101 Homo sapiens clone 23872 mRNA sequence	
0.0006219	370.18	117.99	**3.13737**	potassium inwardly-rectifying channel, subfamily J, member 8	KCNJ8
4.81E-05	129.81	40.39	**3.21409**	enabled homolog (Drosophila)	ENAH
0.000145	79.46	24.66	**3.22186**	tumor necrosis factor, alpha-induced protein 8-like 1	TNFAIP8L1
0.0003862	1558.43	483.34	**3.22430**	BRI3 binding protein	BRI3BP
6.68E-05	53.11	16.20	**3.27799**	membrane metallo-endopeptidase	MME
0.0002503	552.82	156.83	**3.52496**	Transcribed locus	
8.51E-05	138.77	38.12	**3.64070**	CDNA FLJ32526 fis, clone SMINT2000073	

2.31E-05	106.82	28.74	**3.71679**	acyl-Coenzyme A oxidase 1, palmitoyl	ACOX1
0.0002186	877.62	234.87	**3.73653**	myosin VA (heavy chain 12, myoxin)	MYO5A
0.0001549	491.61	131.19	**3.74720**	signal sequence receptor, alpha (translocon-associated protein alpha)	SSR1
0.0009418	92.42	24.22	**3.81644**	potassium channel, subfamily K, member 2	KCNK2
0.0006952	22.80	5.96	**3.82310**	CDNA: FLJ22073 fis, clone HEP11868	
0.0007667	461.21	120.19	**3.83745**	heterogeneous nuclear ribonucleoprotein A0	HNRNPA0
0.000272	1545.94	390.58	**3.95806**	CDNA clone IMAGE:4842353	
0.0005843	123.40	31.17	**3.95842**	prostaglandin E receptor 2 (subtype EP2), 53kDa	PTGER2
0.000281	658.78	164.50	**4.00465**	transmembrane protein 64	TMEM64
8.31E-05	1674.86	413.01	**4.05522**	caveolin 1, caveolae protein, 22kDa	CAV1
0.0006266	61.76	14.80	**4.17301**	NEL-like 2 (chicken)	NELL2
7.78E-05	574.25	137.28	**4.18311**	caveolin 2	CAV2
0.0003611	3974.38	933.07	**4.25946**	caveolin 1, caveolae protein, 22kDa	CAV1
4.68E-05	153.26	35.70	**4.29316**	katanin p60 subunit A-like 1	KATNAL1
6.88E-05	30.01	6.90	**4.35190**	endoplasmic reticulum protein 27 kDa	ERP27
0.0001087	229.94	52.77	**4.35706**	chromosome 20 open reading frame 142	C20orf142
9.07E-05	4627.17	1050.70	**4.40389**	CDNA clone IMAGE:4842353	
0.0002625	239.63	54.24	**4.41754**	GTP binding protein overexpressed in skeletal muscle	GEM
0.0001919	2333.90	508.05	**4.59389**	hypothetical protein LOC143381	LOC143381
0.0001045	452.33	95.14	**4.75416**	transmembrane protein 83	TMEM83
0.0006806	419.80	70.46	**5.95804**	CDNA FLJ33081 fis, clone TRACH2000321	
0.0007229	490.86	79.93	**6.14100**	achaete-scute complex homolog 1 (Drosophila)	ASCL1
0.0004111	68.54	7.13	**9.61311**	CDNA FLJ33081 fis, clone TRACH2000321	
0.0003614	181.41	7.61	**23.83209**	collagen, type XII, alpha 1	COL12A1

Table 4. Primer ID, sequence, usage and source of DNA oligo primers used.

Primer ID	Sequence	Used for	Source
pESR1_1F	CCACCAACCAGTGCACCATT	Real Time PCR	http://web.ncifcrf.gov/rtp/gel/primerdb/
pESR1_1R	GGTCTTTTCGTATCCCACCTTTC	Real Time PCR	http://web.ncifcrf.gov/rtp/gel/primerdb/
hGAPDH-5	ACCCAGAAGACTGTGGATGG	Real Time PCR	(9)
hGAPDH-3	TCTAGACGGCAGGTCAGGTC	Real Time PCR	(9)
p21F	GGACCTGGAGACTCTCA	Real Time PCR	(10)
p21R	CCTCTTGGAGAAGATCAG	Real Time PCR	(10)
PUMAF	GACCTCAACGCACAGTA	Real Time PCR	(10)
PUMAR	CTAATTGGGCTCCATCT	Real Time PCR	(10)
145_P1F	TGGCAGAACACCTCTCTCCT	CHIP	Predicted by PWM approach
145_P1R	AATGCCCAAAAACTCTGCAC	CHIP	Predicted by PWM approach
145_P2F	GTTGCAAGAATCTGGGGAAA	CHIP	Predicted by PWM approach
145_P2R	GGCATGTTTCGAATTGGAGT	CHIP	Predicted by PWM approach
145_P3F	GTGCCTATTGCACAGTCAGC	CHIP	Predicted by PWM approach
145_P3R	AGACCTGCCCAGCCTAGAAT	CHIP	Predicted by PWM approach
145_P4F	GGGTTCAAACCATTCTCCTG	CHIP	Predicted by PWM approach
145_P4R	GGGGAGCCCTTGTCTCTAAT	CHIP	Predicted by PWM approach
145_P5F	ATGAGCTGTAGCCCAAGAGG	CHIP	Predicted by PWM approach

145_P5F	TCGAGCAATCAATTGTCTCC	CHIP	Predicted by PWM approach
145_P6F	ATGGCATCAAAAGGTAGGTC	CHIP	Predicted by PWM approach
145_P6R	GTGAGTACAATTAACAGG	CHIP	Predicted by PWM approach
145 P7F	AGGTGGGCAGAGAGTAGCAA	CHIP	UCSC
145 P7R	CCCAACCATGATCAACTTCC	CHIP	UCSC
p21_CHIP_F	GCACTCTTGTCCCCCAG	CHIP	(11)
p21_CHIP_R	TCTATGCCAGAGCTCAACAT	CHIP	(11)
miR-34a_P5F	ATACCGCTCGAGCGCCCTGCCTGGCCCCCAC	CHIP	(12)
miR-34a_P5r	ATACCGCTCGAGAGCAGGTAGTGCAGGCTTC	CHIP	(12)
145_ESR1Spe_1F	CTACTAGTATGACCATGACCCTCCACAC	Luciferase	
145_ESR1Spe_1R	CTACTAGTCCTCGGGGTAGTTGTACACG	Luciferase	
145_ESR1Spe_2F	CTACTAGTCCAGATGGTCAGTGCCTTGT	Luciferase	
145_ESR1Spe_2R	CTACTAGTAGTAGCTTCCCTGGGTGCTC	Luciferase	
145_ESR1Spe_3F	CTACTAGTCCCAGCTCCTCCTCATCC	Luciferase	
145_ESR1Spe_3R	CTACTAGTCCTCCCCCGTGATGTAATACT	Luciferase	

Acknowledgments

I would like to thank doc. Milena S. Nicoloso, Laura Lupini, doc. Yiling Lu, Julie Fogarty, Simona Rossi, doc. Barbara Zagatti, doc. Muller Fabbri, Angelo Veronese, doc. Xiuping Liu, doc. Ramana Davuluri, doc. Gordon Mills, doc. Massimo Negrini, doc. George A. Calin and doc. Carlo M. Croce for the help during the realization on the bench and on the paper of my work and my phD thesis, respectively. I would like also to thank Izabela Fokt (Department of Experimental Therapeutics, M.D.Anderson Cancer Center, Houston, TX) for adryamicin synthesis.

REFERENCES

1. Lee Y, Jeon K, Lee JT, Kim S, Kim VN. MicroRNA maturation: stepwise processing and subcellular localization. *The EMBO journal* 2002 Sep 2; 21(17): 4663-4670.

2. Lim LP, Lau NC, Garrett-Engele P, Grimson A, Schelter JM, Castle J*, et al.* Microarray analysis shows that some microRNAs downregulate large numbers of target mRNAs. *Nature* 2005 Feb 17; 433(7027): 769-773.

3. Place RF, Li LC, Pookot D, Noonan EJ, Dahiya R. MicroRNA-373 induces expression of genes with complementary promoter sequences. *Proceedings of the National Academy of Sciences of the United States of America* 2008 Jan 28.

4. Vasudevan S, Tong Y, Steitz JA. Switching from repression to activation: microRNAs can up-regulate translation. *Science (New York, NY* 2007 Dec 21; 318(5858): 1931-1934.

5. Stefani G, Slack FJ. Small non-coding RNAs in animal development. *Nat Rev Mol Cell Biol* 2008 Mar; 9(3): 219-230.

6. Voorhoeve PM, Agami R. Classifying microRNAs in cancer: the good, the bad and the ugly. *Biochimica et biophysica acta* 2007 Jun; 1775(2): 274-282.

7. O'Donnell KA, Wentzel EA, Zeller KI, Dang CV, Mendell JT. c-Myc-regulated microRNAs modulate E2F1 expression. *Nature* 2005 Jun 9; 435(7043): 839-843.

8. He L, He X, Lowe SW, Hannon GJ. microRNAs join the p53 network--another piece in the tumour-suppression puzzle. *Nature reviews* 2007 Nov; 7(11): 819-822.

9. Yamakuchi M, Ferlito M, Lowenstein CJ. miR-34a repression of SIRT1 regulates apoptosis. *Proceedings of the National Academy of Sciences of the United States of America* 2008 Sep 9; 105(36): 13421-13426.

10. Tazawa H, Tsuchiya N, Izumiya M, Nakagama H. Tumor-suppressive miR-34a induces senescence-like growth arrest through modulation of the E2F pathway in human colon cancer cells. *Proceedings of the National Academy of Sciences of the United States of America* 2007 Sep 25; 104(39): 15472-15477.

11. Tsang J, Zhu J, van Oudenaarden A. MicroRNA-mediated feedback and feedforward loops are recurrent network motifs in mammals. *Molecular cell* 2007 Jun 8; 26(5): 753-767.

12. Volinia S, Calin GA, Liu CG, Ambs S, Cimmino A, Petrocca F*, et al.* A microRNA expression signature of human solid tumors defines cancer gene targets. *Proceedings of the National Academy of Sciences of the United States of America* 2006 Feb 14; 103(7): 2257-2261.

13. Lu J, Getz G, Miska EA, Alvarez-Saavedra E, Lamb J, Peck D*, et al.* MicroRNA expression profiles classify human cancers. *Nature* 2005 Jun 9; 435(7043): 834-838.

14. Iorio MV, Ferracin M, Liu CG, Veronese A, Spizzo R, Sabbioni S*, et al.* MicroRNA gene expression deregulation in human breast cancer. *Cancer research* 2005 Aug 15; 65(16): 7065-7070.

15. Michael MZ, O' Connor SM, van Holst Pellekaan NG, Young GP, James RJ. Reduced accumulation of specific microRNAs in colorectal neoplasia. *Mol Cancer Res* 2003; 1(12): 882-891.

16. Yanaihara N, Caplen N, Bowman E, Seike M, Kumamoto K, Yi M*, et al.* Unique microRNA molecular profiles in lung cancer diagnosis and prognosis. *Cancer cell* 2006 Mar; 9(3): 189-198.

17. Foekens JA, Sieuwerts AM, Smid M, Look MP, de Weerd V, Boersma AW*, et al.* Four miRNAs associated with aggressiveness of lymph node-negative, estrogen receptor-positive human breast cancer. *Proceedings of the National Academy of Sciences of the United States of America* 2008 Sep 2; 105(35): 13021-13026.

18. Blenkiron C, Goldstein LD, Thorne NP, Spiteri I, Chin SF, Dunning MJ*, et al.* MicroRNA expression profiling of human breast cancer identifies new markers of tumour subtype. *Genome biology* 2007 Oct 8; 8(10): R214.

19. Jemal A, Siegel R, Ward E, Murray T, Xu J, Thun MJ. Cancer statistics, 2007. *CA Cancer J Clin* 2007 Jan-Feb; 57(1): 43-66.

20. Wang X, Tang S, Le SY, Lu R, Rader JS, Meyers C*, et al.* Aberrant expression of oncogenic and tumor-suppressive microRNAs in cervical cancer is required for cancer cell growth. *PLoS ONE* 2008; 3(7): e2557.

21. Akao Y, Nakagawa Y, Naoe T. MicroRNAs 143 and 145 are possible common onco-microRNAs in human cancers. *Oncology reports* 2006 Oct; 16(4): 845-850.

22. Shi B, Sepp-Lorenzino L, Prisco M, Linsley P, deAngelis T, Baserga R. Micro RNA 145 targets the insulin receptor substrate-1 and inhibits the growth of colon cancer cells. *The Journal of biological chemistry* 2007 Nov 9; 282(45): 32582-32590.

23. Shen WF, Hu YL, Uttarwar L, Passegue E, Largman C. MicroRNA-126 Regulates HOXA9 by Binding to the Homeobox. *Molecular and cellular biology* 2008 May 12.

24. Li Y, Jenkins CW, Nichols MA, Xiong Y. Cell cycle expression and p53 regulation of the cyclin-dependent kinase inhibitor p21. *Oncogene* 1994 Aug; 9(8): 2261-2268.

25. Nakano K, Vousden KH. PUMA, a novel proapoptotic gene, is induced by p53. *Molecular cell* 2001 Mar; 7(3): 683-694.

26. He L, He X, Lim LP, de Stanchina E, Xuan Z, Liang Y*, et al.* A microRNA component of the p53 tumour suppressor network. *Nature* 2007 Jun 28; 447(7148): 1130-1134.

27. Vassilev LT, Vu BT, Graves B, Carvajal D, Podlaski F, Filipovic Z*, et al.* In vivo activation of the p53 pathway by small-molecule antagonists of MDM2. *Science (New York, NY* 2004 Feb 6; 303(5659): 844-848.

28. Wei CL, Wu Q, Vega VB, Chiu KP, Ng P, Zhang T*, et al.* A global map of p53 transcription-factor binding sites in the human genome. *Cell* 2006 Jan 13; 124(1): 207-219.

29. Kulshreshtha R, Ferracin M, Wojcik SE, Garzon R, Alder H, Agosto-Perez FJ*, et al.* A microRNA signature of hypoxia. *Molecular and cellular biology* 2007 Mar; 27(5): 1859-1867.

30. Zhou Y, Ferguson J, Chang JT, Kluger Y. Inter- and intra-combinatorial regulation by transcription factors and microRNAs. *BMC Genomics* 2007 Oct 30; 8(1): 396.

31. Lykkesfeldt AE, Larsen JK, Christensen IJ. Cell cycle analysis of estrogen stimulation and antiestrogen inhibition of growth of the human breast cancer cell line MCF-7. *Breast cancer research and treatment* 1986; 7 Suppl: S83-90.

32. Tay Y, Zhang J, Thomson AM, Lim B, Rigoutsos I. MicroRNAs to Nanog, Oct4 and Sox2 coding regions modulate embryonic stem cell differentiation. *Nature* 2008 Oct 23; 455(7216): 1124-1128.

33. Hossain A, Kuo MT, Saunders GF. Mir-17-5p regulates breast cancer cell proliferation by inhibiting translation of AIB1 mRNA. *Molecular and cellular biology* 2006 Nov; 26(21): 8191-8201.

34. Miranda KC, Huynh T, Tay Y, Ang YS, Tam WL, Thomson AM*, et al.* A pattern-based method for the identification of MicroRNA binding sites and their corresponding heteroduplexes. *Cell* 2006 Sep 22; 126(6): 1203-1217.

35. Grisouard J, Medunjanin S, Hermani A, Shukla A, Mayer D. Glycogen synthase kinase-3 protects estrogen receptor alpha from proteasomal degradation and is required for full transcriptional activity of the receptor. *Molecular endocrinology (Baltimore, Md* 2007 Oct; 21(10): 2427-2439.

36. Jordan VC, O'Malley BW. Selective estrogen-receptor modulators and antihormonal resistance in breast cancer. *J Clin Oncol* 2007 Dec 20; 25(36): 5815-5824.

37. Malkin D, Li FP, Strong LC, Fraumeni JF, Jr., Nelson CE, Kim DH*, et al.* Germ line p53 mutations in a familial syndrome of breast cancer, sarcomas, and other neoplasms. *Science (New York, NY* 1990 Nov 30; 250(4985): 1233-1238.

38. Chang TC, Wentzel EA, Kent OA, Ramachandran K, Mullendore M, Lee KH*, et al.* Transactivation of miR-34a by p53 broadly influences gene expression and promotes apoptosis. *Molecular cell* 2007 Jun 8; 26(5): 745-752.

39. Liu W, Konduri SD, Bansal S, Nayak BK, Rajasekaran SA, Karuppayil SM*, et al.* Estrogen receptor-alpha binds p53 tumor suppressor protein directly and represses its function. *The Journal of biological chemistry* 2006 Apr 14; 281(15): 9837-9840.

40. Mattie MD, Benz CC, Bowers J, Sensinger K, Wong L, Scott GK*, et al.* Optimized high-throughput microRNA expression profiling provides novel biomarker assessment of clinical prostate and breast cancer biopsies. *Molecular cancer* 2006; 5: 24.

41. Adams BD, Furneaux H, White BA. The micro-ribonucleic acid (miRNA) miR-206 targets the human estrogen receptor-alpha (ERalpha) and represses ERalpha messenger RNA and protein expression in breast cancer cell lines. *Molecular endocrinology (Baltimore, Md* 2007 May; 21(5): 1132-1147.

42. Zhao JJ, Lin J, Yang H, Kong W, He L, Ma X*, et al.* MicroRNA-221/222 negatively regulates estrogen receptor alpha and is associated with tamoxifen resistance in breast cancer. *The Journal of biological chemistry* 2008 Nov 7; 283(45): 31079-31086.

43. Schmittgen TD, Lee EJ, Jiang J. High-throughput real-time PCR. *Methods Mol Biol* 2008; 429: 89-98.

44. Cimmino A, Calin GA, Fabbri M, Iorio MV, Ferracin M, Shimizu M*, et al.* miR-15 and miR-16 induce apoptosis by targeting BCL2. *Proceedings of the National Academy of Sciences of the United States of America* 2005 Sep 27; 102(39): 13944-13949.

45. Tibes R, Qiu Y, Lu Y, Hennessy B, Andreeff M, Mills GB*, et al.* Reverse phase protein array: validation of a novel proteomic technology and utility for analysis of primary leukemia specimens and hematopoietic stem cells. *Molecular cancer therapeutics* 2006 Oct; 5(10): 2512-2521.